

8-2017

CONTRASTING EFFECTS OF AN MDM2 FUNCTIONAL POLYMORPHISM ON TUMOR PHENOTYPES

Guadalupe J. Ortiz IV

Follow this and additional works at: https://digitalcommons.library.tmc.edu/utgsbs_dissertations



Part of the [Medicine and Health Sciences Commons](#)

Recommended Citation

Ortiz, Guadalupe J. IV, "CONTRASTING EFFECTS OF AN MDM2 FUNCTIONAL POLYMORPHISM ON TUMOR PHENOTYPES" (2017). *The University of Texas MD Anderson Cancer Center UTHealth Graduate School of Biomedical Sciences Dissertations and Theses (Open Access)*. 804.
https://digitalcommons.library.tmc.edu/utgsbs_dissertations/804

This Dissertation (PhD) is brought to you for free and open access by the The University of Texas MD Anderson Cancer Center UTHealth Graduate School of Biomedical Sciences at DigitalCommons@TMC. It has been accepted for inclusion in The University of Texas MD Anderson Cancer Center UTHealth Graduate School of Biomedical Sciences Dissertations and Theses (Open Access) by an authorized administrator of DigitalCommons@TMC. For more information, please contact digitalcommons@library.tmc.edu.

**CONTRASTING EFFECTS OF AN *MDM2* FUNCTIONAL POLYMORPHISM
ON TUMOR PHENOTYPES**

By

Guadalupe Javier Ortiz IV, M.S.

APPROVED:

Guillermina Lozano, Ph.D.
Advisory Professor

David G. Johnson, Ph.D.

Pierre McCrea, Ph.D.

Xiaobing Shi, Ph.D.

Sean M. Post, Ph.D.

APPROVED:

Dean, The University of Texas
MD Anderson Cancer Center UTHHealth Graduate School of Biomedical Sciences

**CONTRASTING EFFECTS OF AN *MDM2* FUNCTIONAL POLYMORPHISM ON TUMOR
PHENOTYPES**

A

DISSERTATION

Presented to the Faculty of

The University of Texas

MD Anderson Cancer Center UTHealth

Graduate School of Biomedical Sciences

in Partial Fulfillment

of the Requirements

for the Degree of

DOCTOR OF PHILOSOPHY

by

Guadalupe Javier Ortiz IV, M.S.

Houston, Texas

June 2017

Dedication

This dissertation is dedicated to my mother:

Graciela Segura

For her love and guidance

Acknowledgments

I am very thankful to all the people who have supported me in throughout my graduate education. I thank my mother for instilling persistence in me and for all her dedication and encouragement. I thank my sister for all her support and for being a role model in my life. To my wife Nazila, who is my everything, I appreciate you and I thank you for all your love and support.

I am eternally grateful to my mentor, Dr. Gigi Lozano. I would like to thank her for the opportunity and support she provided me to further my potential as a scientist. Thank you for everything you have done for me. I would also like to thank my lab members for all their guidance and support but above all, their friendship.

I also appreciate all the staff from GSBS and Genes and Development program for their support towards the completion of my degree. They have been like family to me. Finally, my friends, you guys are awesome, thank you!

Abstract

Contrasting effects of an *Mdm2* functional polymorphism on tumor phenotypes

Guadalupe Javier Ortiz IV, M.S.

Advisory Professor: Guillermina Lozano, Ph.D.

Cancer predisposition by the cooperation of genetic variants, such as single nucleotide polymorphisms (SNPs), may be of much greater significance to public health than previously appreciated. Functional polymorphisms are genetic variants that alter gene function. Meta-analyses associate many functional polymorphisms with cancer risk. The *MDM2* *SNP309G* allele is a cancer-associated functional polymorphism positioned in the *MDM2* P2 promoter that enhances transcription factor SP1 binding, resulting in elevated levels of MDM2 concomitant with decreased p53 tumor-suppressor activity. *Mdm2*^{*SNP309G/G*} mice are more prone to spontaneous tumor formation than *Mdm2*^{*SNP309T/T*} mice, providing direct evidence for the impact of this SNP on tumor development. We examined the impact of *SNP309* on cancer risk in response to environmental factors by treating *SNP309* mice with ionizing radiation, UVB, or Benzo(a)pyrene. The results show that *SNP309G* cooperates with ionizing radiation to exacerbate tumor development. Contrastingly, ultraviolet B light or Benzo(a)pyrene exposure of skin indicates that *SNP309G* allele *protects* against squamous cell carcinoma susceptibility. These contradicting differences led us to interrogate the mechanism by which *Mdm2* *SNP309* regulates tumor susceptibility in a tissue-specific manner. The assessment of potential transcriptional regulators in ENCODE ChIP-seq database identified transcriptional

repressor E2F6 as a possible negative regulator of *MDM2* expression. Our data show that E2F6 protein is expressed at higher levels in skin keratinocytes of *SNP309* mice as compared to lymphatic tissues. Furthermore, E2F6 binds and suppresses *Mdm2* expression in cells harboring the *SNP309G* allele but not the *SNP309T* allele. Thus, the *Mdm2 SNP309G* allele exhibits tissue-specific regulation and differentially impacts cancer risk.

Table of Contents

Approval Sheet.....	i
Title Page.....	ii
Dedication	iii
Acknowledgments	iv
Abstract	v
Table of Contents	vii
List of Illustrations	xi
List of Tables.....	xiv
Chapter 1. Introduction	2
The guardian of the genome.....	2
Discovery and characterization of the p53 protein.....	2
p53 activation	3
Tumor suppressor function.....	4
p53 regulators.....	6
Mdm2: p53 regulator.....	6
Mdm2 transcriptional regulation.....	7
Mdm4 is a regulator of p53	9
Attenuating the p53 pathway in human cancers.....	9
Haploinsufficiency of <i>Mdm2</i> and <i>Mdm4</i> in tumor development	10
Single nucleotide polymorphisms (SNPs).....	11
SNPs and disease.....	12
Functional SNPs.....	12
SNPs in the p53 pathway	15

TP53 codon 72	15
MDM2 SNP309 discovery and characterization.....	16
MDM2 SNP309 is associated with cancer risk.....	16
MDM2 SNP309 and association studies.....	17
MDM2 SNP309 mechanism	18
Evidence that SNP309G may exhibit a protective role in cancer	19
Gene-environment interactions and disease risk.....	20
SNP-environmental interactions and cancer risk	21
Hypotheses and Rational	22
Chapter 2. Results	24
Low-dose ionizing radiation preferably attenuates p53 activity in tissues from <i>Mdm2</i> ^{SNP309G/G} mice compared to <i>Mdm2</i> ^{SNP309T/T} mice	25
Low-dose ionizing radiation exacerbates tumor development in <i>Mdm2</i> ^{SNP309G/G} mice compared to <i>Mdm2</i> ^{SNP309T/T} mice.....	30
Low-dose ionizing radiation exacerbates lymphoma development in <i>Mdm2</i> ^{SNP309G/G} mice compared to <i>Mdm2</i> ^{SNP309T/T} mice.....	39
Interim summary	42
Investigating the influence of Ultraviolet radiation on <i>Mdm2</i> ^{SNP309} skin cancer risk ...	43
Ultraviolet radiation preferably attenuates p53 activity in epidermis tissue from <i>Mdm2</i> ^{SNP309T/T} mice compared to <i>Mdm2</i> ^{SNP309G/G} mice	44
Ultraviolet radiation exacerbates squamous cell carcinoma development in <i>Mdm2</i> ^{SNP309T/T} mice compared to <i>Mdm2</i> ^{SNP309G/G} mice	48
Ultraviolet radiation increases <i>Mdm2</i> expression in a tissue-dependent manner in <i>Mdm2</i> ^{SNP309} mice	50

Epidermal tissue from <i>Mdm2</i> ^{SNP309T/T} mice exhibit higher <i>Mdm2</i> expression independent of insult compared to <i>Mdm2</i> ^{SNP309G/G} mice	52
Interim summary	59
Investigating the role of the <i>SNP309G</i> allele in <i>Mdm2</i> regulation in a tissue-dependent manner	60
<i>Mdm2</i> expression is tissue-dependent in <i>Mdm2</i> <i>SNP309</i> mice	60
The identification of E2F family members as transcriptional regulators of the <i>Mdm2</i> gene	65
Transcriptional repressor E2F6 negatively regulates <i>Mdm2</i> expression in <i>SNP309G</i> cells but not in <i>SNP309T</i> cells	69
Transcriptional repressor E2F6 preferably binds to the <i>Mdm2</i> P2 promoter of <i>SNP309G</i> keratinocytes compared to <i>SNP309T</i> keratinocytes	75
Interim summary	77
Chapter 3. Materials and Methods	79
Generation of homozygous <i>Mdm2</i> ^{SNP309T/T} and <i>Mdm2</i> ^{SNP309G/G} mice. (Resource previously available in the laboratory)	79
Environmental stress treatments	80
Histopathology and Immunohistochemistry	81
Western Blot analysis	82
Real-Time RT-PCR	82
Primary cell cultures	83
Chromatin immunoprecipitation assay	84
Statistical analysis	85
Chapter 4. Discussion and Future Directions	87

Discussion	87
<i>Mdm2</i> expression differences in tumor-prone tissues	88
The <i>SNP309G</i> allele cooperates with epidermal cell factors to regulate <i>Mdm2</i> expression in skin tissue.....	91
Clinical implications	92
Future directions.....	94
Characterizing factors that affect SNP-dependent mechanism	94
Summary	95
Bibliography.....	96
Vita	123

List of Illustrations

Figure 1. p53 is a transcription factor that exerts its tumor-suppressor functions by binding to sequence-specific sites in targeting genes.....	5
Figure 2. The p53 and Mdm2 form a feedback loop.....	8
Figure 3. Functional SNP alters gene regulation through multiple mechanisms	14
Figure 4. <i>Mdm2</i> expression in spleen tissues of <i>Mdm2</i> ^{SNP309} mice 3h post IR.....	27
Figure 5. Expression analysis of p53 targets in spleen tissues of <i>Mdm2</i> ^{SNP309} mice 3h post IR.....	28
Figure 6. Immunohistochemistry of spleens and thymi of <i>Mdm2</i> ^{SNP309T/T} and <i>Mdm2</i> ^{SNP309G/G} mice with caspase-3 antibody.....	29
Figure 7. Tumor-free survival curves of <i>Mdm2</i> ^{SNP309} mice comparing non-irradiated and irradiated mice.....	32
Figure 8. Tumor-free survival of non-irradiated <i>Mdm2</i> ^{SNP309} mice.....	33
Figure 9. Tumor-free survival of gamma-irradiated <i>Mdm2</i> ^{SNP309} mice	34
Figure 10. Tumor incidence in gamma-irradiated <i>Mdm2</i> ^{SNP309} mice	36
Figure 11. Tumor multiplicity of <i>Mdm2</i> ^{SNP309} C57BL/6 mice cohort	38
Figure 12. Lymphoma-free survival of gamma-irradiated <i>Mdm2</i> ^{SNP309} mice	40
Figure 13. Lymphomas in <i>Mdm2</i> ^{SNP309G/G} mice exhibit either T-cell or B-cell cell-type.	41
Figure 14. <i>Mdm2</i> expression in <i>Mdm2</i> ^{SNP309} keratinocytes 24h post UV radiation	46
Figure 15. Expression analysis of p53 targets in <i>Mdm2</i> ^{SNP309} skin tissues 24h post UVB.	47
Figure 16. Tumor-free survival of UVB-irradiated <i>SNP309</i> mice.	49

Figure 17. <i>Mdm2</i> expression in <i>Mdm2</i> ^{SNP309} primary fibroblasts cells from FVB mice 24h post UV radiation	51
Figure 18. <i>Mdm2</i> expression in <i>Mdm2</i> ^{SNP309} epidermis tissues 24h post B(a)P treatment.	54
Figure 19. Tumor-free survival of B(a)P treated <i>Mdm2</i> ^{SNP309} mice	55
Figure 20. Tumor-free survival of B(a)P treated <i>Mdm2</i> ^{SNP309} mice separated by gender.	56
Figure 21. <i>Mdm2</i> expression in epidermis tissues of male and female <i>Mdm2</i> ^{SNP309} mice 24h post B(a)P treatment	57
Figure 22. Expression analysis of p53 targets in male <i>SNP309</i> skin tissues 24h post B(a)P treatment	58
Figure 23. <i>Mdm2</i> basal expression in tissues of <i>SNP309</i> mice in C57BL/6 strain	62
Figure 24. <i>Mdm2</i> basal expression in epidermis of <i>SNP309</i> mice in FVB strain.....	63
Figure 25. <i>Mdm2</i> basal expression in <i>SNP309</i> mouse by gender	64
Figure 26. Predicted SP1 & E2F binding sites in the <i>MDM2</i> P2 promoter proximal to <i>SNP309</i> site	66
Figure 27. ENCODE ChIP-seq transcription factor binding analysis proximal to position 309 in the <i>MDM2</i> -P2 promoter	67
Figure 28. Sequencing MCF10A and K562 cell lines for the <i>Mdm2</i> <i>SNP309</i>	68
Figure 29. <i>Mdm2</i> mRNA expression in MEFs transfected with SP1	70
Figure 30. <i>Mdm2</i> mRNA expression in MEFs transfected with E2F4	71
Figure 31. <i>Mdm2</i> mRNA expression in MEFs transfected with E2F6	72
Figure 32. <i>Mdm2</i> mRNA expression in MEFs transfected with SP1 or E2F6.	73
Figure 33. Protein analyses in thymi and keratinocytes of <i>SNP309</i> mice.	74

Figure 34. E2F6 ChIP analysis of the <i>MDM2</i> P2 promoter in keratinocytes of <i>Mdm2</i> ^{SNP309T/T} and <i>Mdm2</i> ^{SNP309G/G} mice.	76
---	----

List of Tables

Table 1. Tumor spectrum in non-irradiated *Mdm2*^{SNP309} mice35

Table 2. Tumor spectrum of *Mdm2*^{SNP309} C57BL/6 mice after 1Gy IR. 37

CHAPTER I
INTRODUCTION

Chapter 1. Introduction

The guardian of the genome

The *TP53* gene is a tumor suppressor that encodes the p53 phosphoprotein, a transcription factor that is paramount in maintaining genome integrity through the regulation of cellular pathways. Thus, p53 is known as “the guardian of the genome” [1].

Discovery and characterization of the p53 protein

The p53 protein was first identified in 1979. The first set of experiments conducted in hamster fibroblast cells transformed with simian virus 40 (SV40) identified a host protein with a molecular weight of 53-55 kDa that co-precipitated with SV40 large T-antigen, suggesting that viral components interact with host proteins to alter cell function [2-4]. Independently, other labs corroborated the co-precipitation experiments, but their studies also showed that sera from SV40-infected and transformed mouse cells harbored the 54 kDa protein, which was not detected in uninfected 3T3 cells or normal sera [5-7], characterizing p53 protein as a tumor antigen.

Several groups examined the p53 oncogenic properties by cloning *p53* cDNA into transformed and non-transformed mouse cells. Most laboratories came to the conclusion that p53 was an oncogene because it was able to immortalize cells or transform them when cells were co-transfected with *Ras* V12 plasmid [8-10]. However, subsequent experiments showed that wild-type p53 cDNA was not able to immortalize or transform cells with the *Ras* oncogene, but rather protects against oncogenes [11-13]. Moreover, the

sequencing of human colon tumors showed that the *TP53* gene harbors mutations and exhibits loss of heterozygosity [14]. Finally, *in vivo* studies revealed that *p53*-deficient mice had a propensity for tumor development [15]. Collectively, these data were conclusive in characterizing p53 protein as a tumor suppressor.

The focus then was to understand how p53 functioned as a tumor suppressor. Molecular studies characterized p53 as a transcription factor that regulated genes that play pivotal roles in cell regulation programs [16]. An example is *p21/WAF1*, a gene that plays a role in cell-cycle arrest [17]. Studies show that the p53 protein targets genes through sequence-specific elements harbored within the target promoter [18-21]. Thus, p53 is a transcription factor with potent tumor suppressor activity.

p53 activation

In response to stress signals, p53 transactivates many genes involved in processes that are critical for maintaining genomic stability and cell homeostasis [16]. The p53 protein activates these target genes by binding to specific DNA response elements (RE's) in the promoter as a tetrameric structure [22, 23]. These unique DNA sequences are characterized as two copies of the ten base motifs RRRCWWGYYY (R: purine, W: adenine or thymine, Y: pyrimidine) separated by 0-13 nucleotides [18]. Numerous types of stress factors activate the p53 pathway [24, 25]. In response to ionizing radiation, a source of reactive oxygen species (ROS) and DNA breaks in the genome, p53 is activated via phosphorylation by the kinases ATM (Ataxia Telangiectasia Mutated) and Chk2 [26].

Tumor suppressor function

Many p53 target genes, including *p21* and *puma*, have been identified and play vital roles to mediate p53 functions including cell cycle arrest, DNA repair, and apoptosis [27-30]. The decision of the cell to undergo these programs also depends on the cell type, the levels of stress, and the external environment, which determine the spectrum of p53 activation [24, 25, 31]. In response to slight damage, p53 elicits programs like DNA repair and cell cycle arrest to allow cells to recover and revert to normal. However, in response to robust insult, p53 induces programs to mediate cell death, such as apoptosis or senescence [16]. The p53 pathway elicits other programs that are critical barriers to genomic instability, including but not limited to sensitizing cells to ferroptosis [32], autophagy [33], and altering cell metabolism to promote oxidative stress by inhibiting the glycolysis pathway [34] (Figure 1).

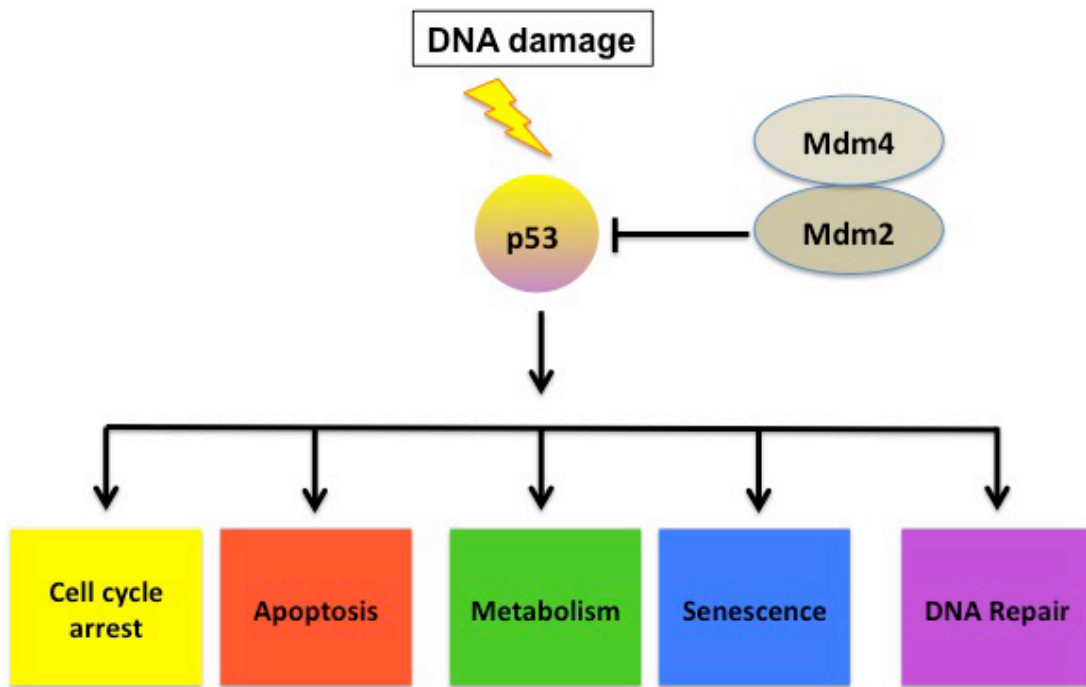


Figure 1. p53 is a transcription factor that exerts its tumor-suppressor functions by binding to sequence-specific sites in targeting genes. Under normal conditions, many regulators tightly regulate the p53 protein. However, in response to cellular stress, the p53 protein orchestrates the transactivation of many genes that activate cellular programs that promote tumor suppressor activity.

p53 regulators

As previously stated, the p53 tumor suppressor protein is critical for maintaining cell homeostasis [35, 36]. Thus, its protein levels and function are tightly regulated. Many negative regulators of p53 have been identified such as Trim24 [37], ARF [38], COP1 [39], and Pirh2 [40]; however, Mdm2 and Mdm4 are the most potent p53 inhibitors [41].

Mdm2: p53 regulator

The *Mdm2* gene was first characterized due to amplification on double minute chromosomes in mouse NIH-3T3 fibroblast cells that provide the cells a growth advantage [42]. *In vivo* studies have concluded that Mdm2 is a potent negative regulator of tumor suppressor p53 protein; mouse models with homozygous *Mdm2* deletions exhibit embryonic lethality, a phenotype that is entirely rescued by *p53* deletion [43, 44]. Moreover, mice lacking *Mdm2* in certain cell-types, including neuronal progenitors, cardiomyocytes, epithelial intestinal cells, and hepatocytes show embryonic lethality, yet these phenotypes are ultimately rescued by *p53* deletion, independent of cell-type [45, 46]. The Mdm2 protein negatively regulates p53 activity by physically binding to the N-terminal transactivation domain (TAD) and hindering p53 transactivation potential [47, 48]. Also, the Mdm2 RING-domain exhibits E3 ubiquitin ligase activity which ubiquitinates p53 and targets it for proteasomal degradation [49-51].

Mdm2 transcriptional regulation

The *Mdm2* gene harbors two promoters: a p53-independent promoter (P1) and a p53-dependent promoter (P2), which is located in intron 1 of the *Mdm2* gene [50]. Expression from the P1 and P2 promoters encode the same full-length protein [52, 53]. However, the translation potential from the P2 promoter is eight-times higher compared to the P1 transcript [54].

In response to DNA damage, the p53 protein binds to p53-responsive elements within the P2 promoter and promotes p53-dependent *Mdm2* transactivation [55-57], thus establishing a negative feedback loop. The importance of the Mdm2-p53 interactions in response to DNA damage was further established *in vivo*. Mice harboring mutations in the p53 response elements within the *Mdm2* P2 promoter are viable with no apparent phenotypes [57]. However, when challenged with DNA damage, the mice are radiosensitive and exhibit a p53-dependent myeloablation and subsequent lethality [57]. Thus, the p53-Mdm2 feedback loop is required to regulate p53 in response to stress (Figure 2).

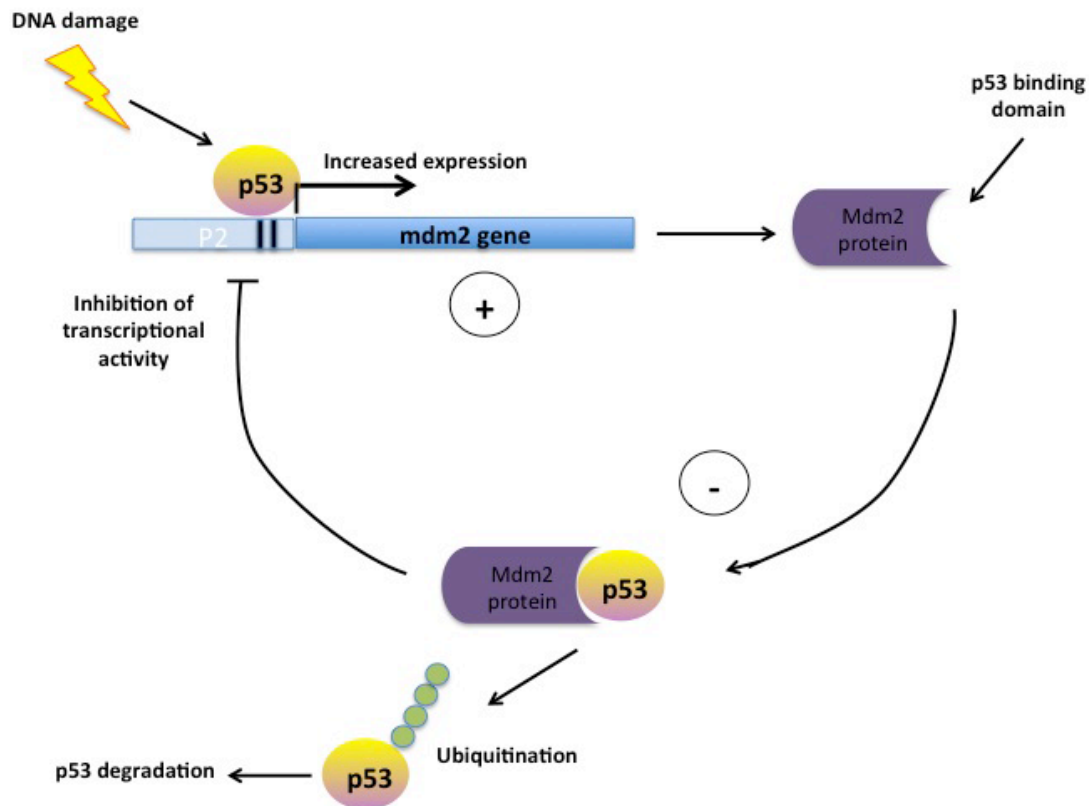


Figure 2. p53 and Mdm2 form a feedback loop. Under cellular stress, p53 is stabilized, thus increasing p53 activity and resulting in upregulation of many p53 target genes that promote tumor suppressor activity. The p53-mediated activation of *MDM2* transcription generates MDM2 protein that causes MDM2-mediated ubiquitination and degradation of p53.

Mdm4 is a regulator of p53

The *Mdm4* gene encodes a 490-amino acid protein that shares similarities with its homolog Mdm2 [58]. Mdm4 harbors a similar C-terminal RING domain, but it does not exhibit E3 ligase activity [58]. Biochemical studies also show that Mdm4 forms a complex with the p53 protein and blocks its transactivation activity [59]. Similarly to the *in vivo* *Mdm2* studies, homozygous *Mdm4* deletions in mice exhibit embryonic lethality, a phenotype that is entirely rescued by *p53* deletion [60-62]. Together, these data conclude that Mdm4 is a potent negative regulator of p53 activity.

Attenuating the p53 pathway in human cancers

TP53 is the most highly altered gene in human cancers with more than 50% harboring mutations [63, 64]. Studies investigating Li-Fraumeni syndrome (LFS), a rare genetic disorder characterized by predisposition to tumor development, revealed that inherited *TP53* mutations were the cause of this familial syndrome [65]. Furthermore, mouse studies harboring p53 mutations also exhibit cancer phenotypes [15, 66]. The p53 pathway can be dampened by additional mechanisms, including amplification or overexpression of genes encoding p53 negative regulators [48, 67, 68]. The *MDM2* gene is amplified and overexpressed in many tumors. Early human studies described *MDM2* gene amplifications in sarcomas [48], but later studies show other tumor types, including glioblastomas, and breast cancer [69]. Another mechanism by which MDM2 is altered in cancers is through overexpression, where it correlates with tumor grade and poor

prognosis in mesothelioma patients [70]. Moreover, tumor studies show a mutually exclusive relationship between MDM2 and p53; tumors harboring *MDM2* amplification seldom carry *TP53* mutations [71, 72], thus suggesting that either alteration dampens p53 activity.

Studies also show that subtle alterations in the p53 pathway can be detrimental to overall survival. A p53 restoration study revealed that mice harboring different levels of p53 activity correlated with overall survival [73]. Expression of as little as 7% difference in p53 expression altered survival [73], thus emphasizing the importance of p53 tumor suppressor activity and gene-dosage effects.

Haploinsufficiency of *Mdm2* and *Mdm4* in tumor development

In addition, minor changes in Mdm2 and Mdm4 levels also impact survival and cancer risk. Mice harboring a hypomorphic *Mdm2* allele that expressed ~30% of Mdm2 protein exhibited elevated levels of p53 activity [74]. These mice were small, radiosensitive, and showed a reduced number of lymphocytes. This phenotype was rescued by p53 deletion. Moreover, these mice are resistant to the development of colorectal cancers in a p53-dependent manner [74].

Genetic studies show that *Mdm2* haploinsufficiency promotes p53 activity [74-76]. Studies examined if the loss of a single *Mdm2* or *Mdm4* allele would affect tumor development. Mouse models overexpressing *Eμ-myc* are susceptible to B cell lymphomas, and often these tumors exhibit Mdm2 overexpression but no gene

amplification [77]. Thus, *Mdm2*^{+/+} or *Mdm2*^{+/-} mice were crossed with *Eμ-myc* transgenic mice and show that *Mdm2* haploinsufficiency delays B-cell lymphomagenesis compared to *Eμ-myc* transgenic harboring wild-type *Mdm2* gene [75]. Another study investigated if reduced levels of Mdm2 or Mdm4 affected p53 response to DNA damage [76]. *Mdm2*^{+/-} and *Mdm4*^{+/-} mice are viable and exhibit a normal phenotype. However these animals were radiosensitive, exhibiting reduced levels of lymphocytes in the blood, and ultimately dying in response to a sub lethal dose of ionizing radiation [76]. Furthermore, double heterozygous *Mdm2*^{+/-} mice *Mdm4*^{+/-} mice show defects in hematopoiesis and brain development and are not viable, a phenotype that is rescued by deleting a single p53 allele [76]. Collectively, these data highlight the delicate balance within the p53 pathway and suggest that the balance could be tissue-dependent.

Single nucleotide polymorphisms (SNPs)

Single nucleotide polymorphisms are characterized as nucleotide variants at a particular location of the genome, and these nucleotide differences are present in at least 1% of a population [78]. SNPs are the most common genetic variants in the human genome with a frequency of approximately one in 300 bases, suggesting that there are close to 10 million SNPs in the genome [79, 80]. Due to their high frequency, SNPs are used as biological reference points in the genome, and this information can be used to measure evolutionary changes in genes of interest [79]. Furthermore, SNPs are relevant in studying human health.

SNPs and disease

There is a wealth of evidence associating single nucleotide polymorphisms (SNPs) and disease susceptibility [81-83]. Meta-analysis studies evaluate associations between inherited deleterious alleles and disease risk [84, 85]. A recurrent issue in the meta-analysis is the consistency in associating SNPs and disease risk within study groups, where studies often report contradicting findings [86, 87]. One obvious reason is that most SNPs used in association studies are not well characterized, so their function and detailed mechanisms behind disease risk are poorly understood. Therefore, it is important to understand the functional role of SNPs to analyze better and associate its role in disease risk.

Functional SNPs

Most SNPs are located in noncoding sequences or in non-regulatory regions of the DNA, which limits their potential to disrupt gene function or cause deleterious effects on health or development; these SNPs are called synonymous substitutions or silent substitutions [88]. Functional SNPs are non-synonymous substitutions that are positioned within regulatory or protein coding sequences and can alter gene expression or protein structure, thus altering function and contributing to disease risk [89-94].

Functional SNPs located within promoters or enhancers alter gene expression. An example is FLT1-T, a SNP located in the promoter region of *flt-1* within a p53-responsive element site [89]. *Flt-1* is a target of VEGF and associated with tumor

progression. Studies show that in response to induced DNA damage, p53 protein binds to the FLT1-T but not the FLT1-C promoter [89]. Thus, the FLT1-T SNP directly affects p53-mediated transcription in the *flt-1* gene.

Another example is MYC-335, an enhancer located upstream of the MYC gene that harbors SNP rs6983267, and associates with cancer risk, including colorectal cancer [94]. The “G” allele creates a stronger binding site for transcription factor TCF4 compared to the “T” allele, thus increasing expression of the *MYC* oncogene [95]. In vivo studies showed that mice lacking this enhancer exhibit a modest decrease in *MYC* mRNA in intestinal crypts and are resistant to intestinal tumors, suggesting that SNP rs6983267 plays a direct role in tumor risk [94].

Finally, functional polymorphisms can alter gene regulation by modulating alternative splicing. Reduced expression levels of Lysyl oxidase-like 1 (*LOXLI*) are associated with risk for pseudoexfoliation (PEX) syndrome [96]. A functional polymorphism (rs11638944) located downstream of the canonical *LOXLI* promoter (intron 2) reduces the expression levels of *LOXLI*, mediated by modulating alternative splicing of *LOXLI* and concomitantly reduced levels of *LOXLI* mRNA in cells and tissues of risk allele carriers [96]. Experiments concluded that alternative splicing of *LOXLI* pre-mRNA coupled with nonsense-mediated decay is significantly influenced by this SNP, which is near the splice site [96]. Thus, functional SNPs can affect gene regulation through multiple mechanisms (Figure 3).

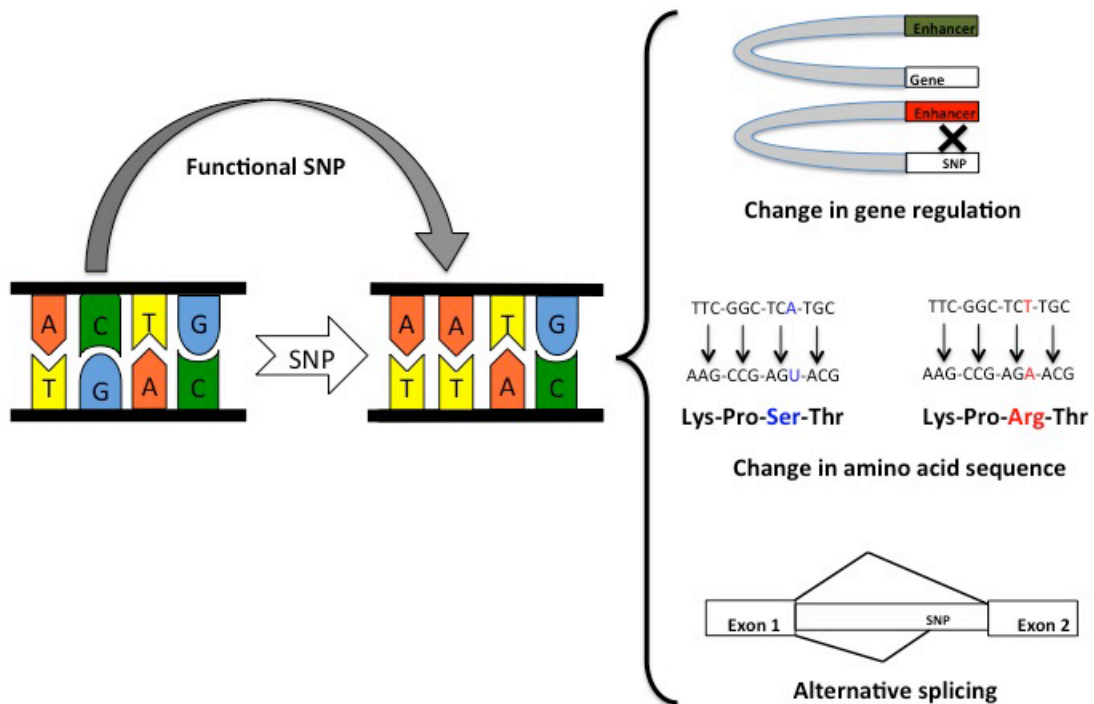


Figure 3. Functional SNP alters gene regulation through multiple mechanisms. The SNPs are naturally occurring genetic variation in the genome. SNPs occurring in regulatory elements alter gene function and may cause disease.

SNPs in the p53 pathway

The p53 pathway regulates many cellular programs that limit tumorigenesis potential in vertebrates [97, 98]; thus, the attenuation of this pathway increases tumor risk and creates a poor outcome [99]. Several studies show that functional polymorphisms harbored within genes involved in the p53 pathway, including *TP53* and *MDM2*, alter gene function and affect the p53 tumor suppressor activity and modulate tumor risk in humans [100, 101]. Most mechanisms involving SNPs in the p53 pathway have not been fully elucidated. Insight into these functional mechanisms could render crucial information that could improve therapeutic targets and human health.

TP53 codon 72

One of the most studied SNPs in the p53 pathway is SNP rs1042522 (also known as p53 codon 72); It is located within the polyproline region in the *TP53* gene [102]. The alleles (C/G) at this locus encode either a proline or arginine residue [103]. Meta-analyses associate P72 with cancer risk [104, 105]. Studies show that SNP rs1042522 affects the p53 activity discretely. *In vivo* studies show that mice harboring P72 exhibit increased growth arrest when challenged with DNA damage due to enhanced p53 binding to the *p21* gene [106]. Contrastingly, mice harboring R72 exhibit increased apoptotic response when tested with DNA damage [106]. Furthermore, R72 structural conformation in p53 enhances the transactivation of pro-apoptotic genes [106]. Together, these data show that functional SNPs alter gene activity.

MDM2 SNP309 discovery and characterization

The *MDM2*^{SNP309} polymorphism was identified in an investigation that characterized genetic variants in the *MDM2* P2 promoter region. The study utilized genomic DNA from 50 healthy individuals and analyzed the P2 promoter and found that at position 309 there is a nucleotide substitution from T to G [107]. To examine the functional consequences of this SNP, bioinformatics and molecular biology analyses demonstrated that the *SNP309G* allele created a preferred binding site for transcription factor SP1. Moreover, an analysis in cell lines that harbored homozygous *SNP309G* alleles exhibited higher *MDM2* expression levels compared to homozygous *SNP309T* cells, concomitantly attenuating p53 activity [107]. Thus, *MDM2 SNP309G* is functional polymorphism that alters the p53 pathway.

MDM2 SNP309 is associated with cancer risk

MDM2 SNP309G is a functional polymorphism in the p53 pathway that associates with increased cancer risk in many cancer types, including lung, colon, pancreas, endometrium, and head and neck [107-111]. The first association of the *MDM2*^{SNP309} polymorphism with increased tumor risk was in Li-Fraumeni syndrome (LFS) patients. The authors hypothesized that because *SNP309G* dampen p53 tumor suppressor activity, LFS patients harboring the *SNP309G* allele would be more prone to tumor risk compared to *SNP309T* individuals. The data show that the *SNP309G* allele was associated with a 10-year earlier onset of breast tumors compared to the *SNP309T* allele in LFS patients [107]. Moreover, LFS patients harboring homozygous *SNP309G*

alleles exhibited more tumors compared to *SNP309T* individuals [107]. Thus, the “G” allele may exacerbate tumor susceptibility in LFS patients by increasing *MDM2* levels to further attenuate p53 tumor suppressor activities.

MDM2 SNP309 and association studies

Although the *SNP309G* allele is highly associated with increased cancer risk, some published studies are inconclusive [108, 112]. For example, several reports show a strong association of *SNP309G* allele with lung cancer risk in the Chinese population [113, 114]; however, studies conducted with American-born subjects show no association between *SNP309G* allele and lung cancer risk [115]. These contradicting data suggest that other factors, including race, may impact *SNP309G*-dependent cancer risk. Race is exemplified in a study that showed that genetic variant *SNP285C*, a SNP harbored within the *MDM2* P2 promoter and only expressed in Caucasians, antagonizes the *SNP309G* allele cancer risk and protects against breast, ovarian, and endometrial cancers [116, 117]. However, the *SNP285C* allele did not antagonize the effect of the *SNP309G* allele on prostate cancer risk [116], suggesting that the *SNP285C* allele may be factor-dependent. Meta-analyses suggest that gender impacts *SNP309G*-dependent cancer risk. For example, a study associating *SNP309G* with lung cancer risk indicate that homozygous G alleles raised lung cancer risk among females [112]. A second study associating *SNP309G* with osteosarcoma showed that female osteosarcoma patients exhibited significantly increased risk (GG versus TT; odds ratio, 4.26; 95% CI, 1.61-11.25) [118]. These studies show the association of *MDM2 SNP309G* with cancer risk in females

MDM2 SNP309 mechanism

Mechanistically the *SNP309G* sequence creates a stronger binding site for the transcription factor SP1 in the *MDM2* P2 promoter [107]. SP1 is a zinc finger that binds to GC-rich regions and is a potent transcriptional activator [116]. *In vitro* studies measured the binding affinity of SP1 to DNA fragments containing either the *SNP309G* or the *SNP309T* allele. The data concluded that the affinity was modestly higher in the *SNP309G* allele (~22%) compared to the *SNP309T* allele [117]. However, this difference is enough to significantly increase *MDM2* mRNA expression levels in cells harboring the *SNP309G* compared to the *SNP309T* allele and concomitantly decrease p53 activity [107].

To investigate the direct impact of *SNP309G* on tumor risk, genetically engineered mice harboring the *Mdm2* *SNP309* alleles were generated and evaluated for tumor susceptibility. A comparison of human and mouse promoter sequences showed weak conservation (82%) and absence of the *Mdm2* *SNP309* [119]. Therefore, *Mdm2*^{*SNP309G/G*} and *Mdm2*^{*SNP309T/T*} mice were generated by replacing the mouse intron 1 (containing the entire P2 promoter) with the corresponding human intron 1 with either the G or T polymorphism [119]. These models facilitate an analysis of the direct impact of *Mdm2* P2 promoter *SNP309* on transcriptional regulation.

First, the authors evaluated the effect of the *SNP309G* allele on *Mdm2* expression and p53 tumor suppressor activity. Lymphatic tissues, including thymi and spleen, harvested from *Mdm2*^{*SNP309G/G*} mice show significantly higher *Mdm2* expression levels compared to *Mdm2*^{*SNP309T/T*} tissues [119]. Consistently, brain and uteri from

Mdm2^{SNP309G/G} mice also show relatively higher *Mdm2* expression compared to *Mdm2*^{SNP309T/T} tissues, but those data were not statistically significant. The authors also examined the effects of SP1 on *Mdm2* expression in *SNP309* tissues. The data show that spleens from *Mdm2*^{SNP309G/G} mice exhibited decreased *Mdm2* expression levels after treatment with Mithramycin A, a known SP1 inhibitor, but there was no effect on *Mdm2* expression in spleens from *Mdm2*^{SNP309T/T} mice [119]. To analyze the effects of *Mdm2*^{SNP309G} on p53 activity, spleen tissues from *SNP309* mice were treated with 1Gy of ionizing radiation (IR) and evaluated for apoptotic response 3-hours post IR. The data show that spleens from *Mdm2*^{SNP309G/G} mice exhibited decreased apoptotic response compared to *Mdm2*^{SNP309T/T} mice [119]. Thus the p53 pathway is attenuated in tissues from *Mdm2*^{SNP309G/G} mice. Finally, *Mdm2*^{SNP309G/G} mice are more susceptible to spontaneous tumor formation and exhibit a significantly lower overall survival compared to *Mdm2*^{SNP309T/T} mice [119]. These data confirm that the *SNP309G* allele is the “at risk” allele in tumor studies.

Evidence that SNP309G may exhibit a protective role in cancer

Recent studies have identified a protective role of *SNP309G* in some cancers [108]. For example, multiple studies that included Asian and Caucasian cohorts associate the *SNP309G* allele with a decreased risk and late onset of prostate cancer compared to patients harboring the *SNP309T* allele [108, 120]. In these studies, the authors discussed the possibility that hormones may influence the *SNP309G* allele effects on prostate tumor risk. However, this question has not been experimentally tested [120]. There is some

evidence to support that gender influences *SNP309G* dependent tumor risk. One study shows that female melanoma patients harboring homozygous *SNP309G* alleles exhibited a later onset compared to those harboring homozygous *SNP309T* alleles [121].

A recent study evaluated the influence of the *MDM2*^{*SNP309*} polymorphism in survival outcome of surgically resected Non-small-cell lung carcinoma (NSCLC). Reports show no association between *SNP309G* and lung adenocarcinoma in a Japanese population. However, when lung adenocarcinoma was stratified by pathological stage 1 disease, patients harboring homozygous *SNP309T* alleles exhibited significantly shorter survivals compared to patients harboring homozygous *SNP309G* or heterozygous *SNP309T/G* alleles. Thus the homozygous *SNP309T* allele is a prognostic marker for poorer survival in stage 1 adenocarcinoma in a Japanese cohort. Finally, A recent study demonstrated a decreased risk of developing oral squamous cell carcinoma (OSCC) for the *MDM2 SNP309G* group [122] with pronounced susceptibility in the *MDM2 SNP309T* group, suggesting *MDM2 SNP309G* may be protective in a cell-dependent manner. Collectively, these data suggest that *MDM2 SNP309* appears to differentially impact tumor susceptibility in different cancers for reasons that are currently unknown.

Gene-environment interactions and disease risk

Gene-environment studies focus on understanding and measuring the influence of environmental exposure on disease risk in different cohorts [123]. Genetics and environment contribute to disease risk, but limited studies have examined how these factors interact to promote disease risk. Furthermore, meta-analysis studies that focus on

genetic epidemiology are seldom contradicting [124, 125]. Thus mechanisms examining gene-environment interactions are paramount to precisely delineating their influence in disease causation within a cohort.

SNP-environmental interactions and cancer risk

Genome-wide association studies (GWAS) have been crucial in identifying many genetic variants associated with cancer risk [126, 127]. The addition of environmental exposure to GWAS studies may provide further insight into SNP-dependent cancer risk or other susceptibilities otherwise concealed by heterogeneity in subgroups [128]. Here are several examples.

One study examined the influence of different environmental exposures, including diet, UV, smoking, and alcohol consumption with a panel of SNPs associated with colorectal cancer (CRC) risk in the Malaysian population [129]. The study concluded that out of the 12 SNPs associated with CRC, individuals harboring the "A" allele in SNP rs2069521 were more susceptible to colorectal cancer risk when consuming red meat compared to people on a vegetarian diet [129]. Another study examined the influence of smoking on several SNPs associated with lung cancer [130]. The data show that particular SNPs increase lung cancer risk as well as promote chronic obstructive pulmonary disease, an established risk factor for lung cancer [130]. Finally, a study examined the influence of ultraviolet radiation in SNPs associated with non-melanoma skin cancer (NMSC) risk [131]. Studies suggest that the NMSC etiology may be through an immunosuppression pathway; thus, SNPs in cytokines and signaling molecules

correlated with UV-induced immunosuppression pathway were evaluated [131]. The results show that a genetic variant of IL10 increased the risk of basal cell carcinoma and squamous cell carcinoma [131]. These data show correlations between environmental exposures to SNPs associated with cancer risk, yet these data do not reveal the mechanisms. There is a need to mechanistically understand how environmental factors interact with functional polymorphisms to modulate cancer risk.

Hypotheses and Rational

Studies show that *Mdm2*^{SNP309G/G} mice are more prone to tumor development than *Mdm2*^{SNP309T/T} mice, providing direct data for the impact of the *SNP309G* allele on spontaneous tumor development [119]. Moreover, p53 mutant mice harboring the *SNP309G* allele are more prone to tumors compared to p53 mutant mice with the *SNP309T* allele, suggesting that the *SNP309G* influences p53 mutant mice and promotes cancer risk similar to studies in LFS patients [119]. To better characterize the gene-environment interactions of *SNP309G* in cancer risk, I propose to challenge *SNP309* mice with various environmental factors to examine the influence of *SNP309* in spontaneous tumor development. Ergo, I hypothesize that *Mdm2 SNP309G* cooperates with environmental factors to promote spontaneous tumor development. The goal of my study is to characterize environment-*SNP309G* interactions and to elucidate the mechanism(s) involved in *SNP309G*-dependent tumor development. Thus, I challenged *SNP309* mice with different environmental factors and followed them for tumor formation.

CHAPTER II

RESULTS

Chapter 2. Results

Previous studies determined that *Mdm2*^{SNP309G/G} mice are more prone to spontaneous tumor formation than *Mdm2*^{SNP309T/T} mice [119], providing direct evidence for the impact of this SNP in tumor development. To further characterize the cancer risk potential of the *SNP309G* allele, I treated *Mdm2*^{SNP309T/T} and *Mdm2*^{SNP309G/G} mice in a C57BL/6 background with low-dose ionizing radiation to study the effects of environmental factors on a tumor phenotype in this model; hence, I hypothesized that low-dose ionizing radiation exacerbates tumor development in *Mdm2*^{SNP309G/G} mice compared to *Mdm2*^{SNP309T/T} mice.

Ionizing radiation generates DNA double strand breaks and reactive oxygen species (ROS), direct mediators of p53 activation [132]; furthermore, humans are consistently exposed to low-dose ionizing radiation via cosmic rays and medical imaging procedures [133]. The C57BL/6 strain is appropriate for this experiment due to the extensive use of this strain in ionizing radiation tumor studies [134]. A single dose of 1Gy ionizing radiation was experimentally determined to be representative of low-dose ionizing radiation because it is the minimal dose that cannot induce tumors in a wild-type C57BL/6 strain background [134]. To this end, I generated cohorts of *Mdm2*^{SNP309T/T} and *Mdm2*^{SNP309G/G} mice in a C57BL/6 background, treated them with 1Gy ionizing radiation, and followed them for tumor formation.

Low-dose ionizing radiation preferably attenuates p53 activity in tissues from *Mdm2*^{SNP309G/G} mice compared to *Mdm2*^{SNP309T/T} mice

I first characterized the effect of low-dose IR on *Mdm2* levels and p53 activity in spleens of *Mdm2*^{SNP309T/T} and *Mdm2*^{SNP309G/G} mice in a C57BL/6 background. I evaluated the *Mdm2* expression in spleens from irradiated *Mdm2*^{SNP309T/T} *Mdm2*^{SNP309G/G} mice 3 hours post IR treatment. The spleens of *Mdm2*^{SNP309G/G} mice showed a 7.8-fold increase in *Mdm2* levels ($p < 0.0001$) compared to *Mdm2*^{SNP309T/T} spleens (Figure 4). Previous studies show that spleens of non-irradiated *Mdm2*^{SNP309T/T} mice in a C57BL/6 background also exhibit lower *Mdm2* expression compared to *Mdm2*^{SNP309G/G} mice [119]. As expected, non-irradiated spleen samples from *Mdm2*^{SNP309G/G} mice showed significantly higher *Mdm2* basal levels ($p = 0.005$) as compared to spleens from *Mdm2*^{SNP309T/T} mice (Figure 4). Next, I tested the effects of low-dose IR on p53 activity in spleens from *Mdm2*^{SNP309T/T} *Mdm2*^{SNP309G/G} mice by examining the expression levels of *p53 targets*, *p21* and *Puma*, 3 hours post IR treatment. Consistently, the spleens of *Mdm2*^{SNP309G/G} mice showed a significant attenuated p53 response compared to *Mdm2*^{SNP309T/T} spleens after IR treatment (Figure 5), suggesting that low-dose IR has a stronger effect on spleens of *Mdm2*^{SNP309G/G} mice compared to *Mdm2*^{SNP309T/T} spleens by elevating *Mdm2* levels with concomitant attenuation of the p53 response.

To determine the effects of low-dose IR on cell survival, I examined the onset of apoptosis in lymphatic tissues of *Mdm2*^{SNP309G/G} mice and *Mdm2*^{SNP309T/T} mice post-IR. *Mdm2*^{SNP309G/G} mouse lymphatic tissues exhibit a delay in activation of apoptosis compared to *Mdm2*^{SNP309T/T} after low-dose IR as measured by the number of cells staining

positively for cleaved caspase-3 (Figure 6). At 6 hours post IR, spleen, and thymi from *Mdm2*^{SNP309T/T} mice showed the presence of apoptotic cells compared to none in the same tissues of *Mdm2*^{SNP309G/G} mice indicating a delayed response to IR; however, by 12 hours post IR, spleens, and thymi from *Mdm2*^{SNP309G/G} mice showed increased apoptosis compared to *Mdm2*^{SNP309T/T} tissues.

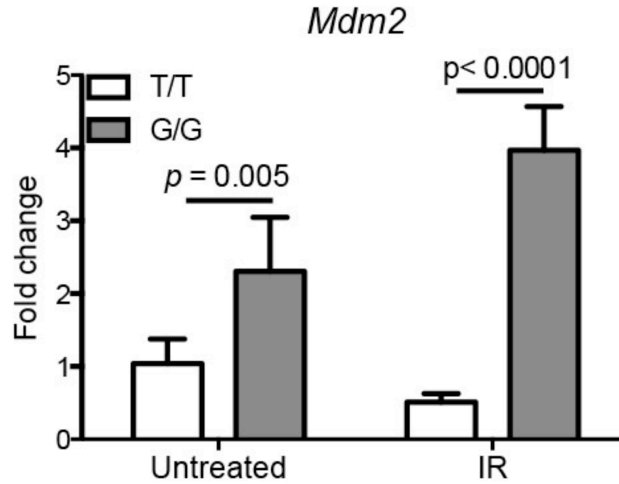


Figure 4. *Mdm2* expression in spleen tissues of *Mdm2*^{SNP309} mice 3h post IR. RT-qPCR analysis of *Mdm2* expression in the spleens of two-day old *Mdm2*^{SNP309T/T} (T/T) and *Mdm2*^{SNP309G/G} (G/G) mice. Five mice per genotype were analyzed. The average expression of untreated (T/T) spleens was normalized to 1 for comparison. *RplpO* expression (housekeeping gene) was used as internal control. IR, ionizing radiation; *Mdm2*^{SNP309T/T}, T/T; *Mdm2*^{SNP309G/G}, G/G.

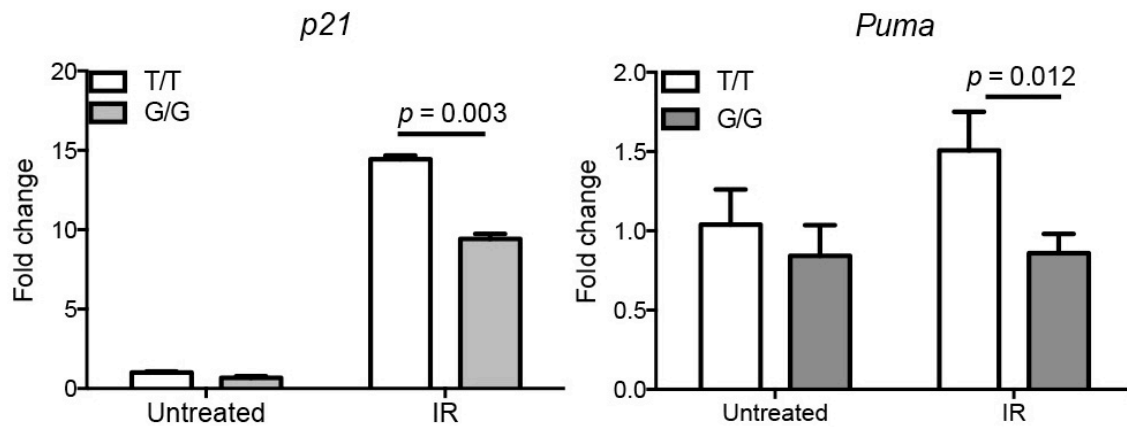


Figure 5. Expression analysis of p53 targets in spleen tissues of *Mdm2*^{SNP309} mice 3h post IR. RT-qPCR expression analysis of *p21* and *puma* in spleens of two-day old *Mdm2*^{SNP309T/T} and *Mdm2*^{SNP309G/G} mice 3 hours post IR treatment (1Gy). Five mice per genotype were analyzed. The average expression of untreated (T/T) spleens was normalized to 1 for comparison. *RplpO* expression (housekeeping gene) was used as internal control. IR, ionizing radiation; *Mdm2*^{SNP309T/T}, T/T; *Mdm2*^{SNP309G/G}, G/G.

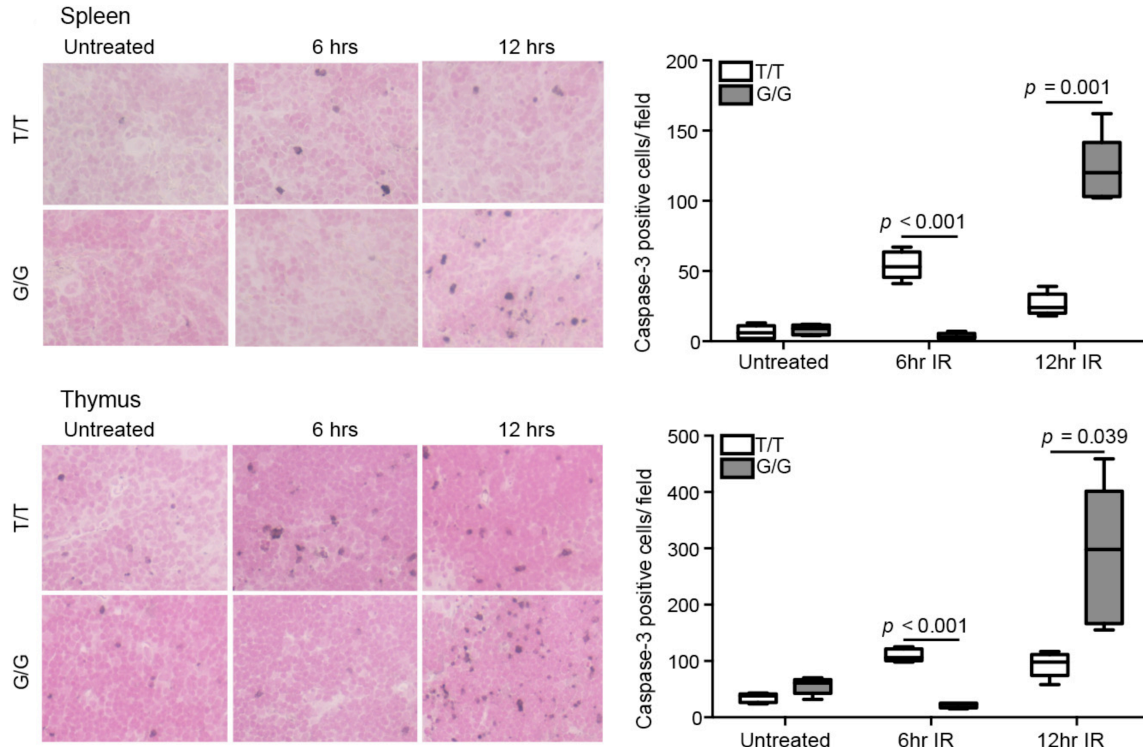


Figure 6. Immunohistochemistry of spleens and thymi of $Mdm2^{SNP309T/T}$ and $Mdm2^{SNP309G/G}$ mice with caspase-3 antibody. The number of positive cells per field of view was counted in three sections per mouse. Graphs represent mean value, $n = 3$, mean \pm SD. Statistical significance was determined by two-way analysis of variance (ANOVA). IR, ionizing radiation; $Mdm2^{SNP309T/T}$, T/T; $Mdm2^{SNP309G/G}$, G/G.

Low-dose ionizing radiation exacerbates tumor development in *Mdm2*^{SNP309G/G} mice compared to *Mdm2*^{SNP309T/T} mice

To examine the long-term effects of low-dose IR on tumor development, I generated a cohort of irradiated *Mdm2*^{SNP309T/T} and *Mdm2*^{SNP309G/G} mice in a C57BL/6 background and monitored for tumor development. I also observed non-irradiated *Mdm2*^{SNP309G/G} and *Mdm2*^{SNP309T/T} mice as controls. The cohort was followed for 850 days (121 weeks). I first analyzed tumor-free survival between non-irradiated and irradiated mice. Tumor-free survival shows that irradiated mice developed significantly more tumors ($p < 0.0001$) than non-irradiated mice independent of genotype (Figure 7). Consistent with previous studies, non-irradiated *Mdm2*^{SNP309G/G} mice are significantly more prone to tumor development ($p < 0.0001$) than non-irradiated *Mdm2*^{SNP309T/T} mice in a C57BL/6 background (Figure 8). Next, I analyzed tumor-free survival between irradiated *Mdm2*^{SNP309G/G} and *Mdm2*^{SNP309T/T} mice and the data show that tumors developed significantly more quickly in irradiated *Mdm2*^{SNP309G/G} mice than in irradiated *Mdm2*^{SNP309T/T} mice ($p < 0.0001$) (Figure 9). *Mdm2*^{SNP309G/G} mice exhibited a median survival of 74 weeks. In contrast, the majority of *Mdm2*^{SNP309T/T} mice survived without tumor development, and thus the median survival could not be calculated.

I analyzed the tumor spectrum in non-irradiated *SNP309* mice (Table 1). The data show that *Mdm2*^{SNP309G/G} have more tumor types compared to *Mdm2*^{SNP309T/T} mice. The tumor types from this study were similar to those previously reported [119]. I then analyzed the tumor incidence in irradiated *Mdm2*^{SNP309G/G} and *Mdm2*^{SNP309T/T} mice. The tumor incidence was significantly higher ($p < 0.0001$) in *Mdm2*^{SNP309G/G} mice compared to

Mdm2^{SNP309T/T} mice (Figure 10). Furthermore, *Mdm2*^{SNP309G/G} mice had a proclivity to develop lymphomas and sarcomas. However, a number of mice also developed other tumors, including mammary carcinomas, glioblastomas, and histiocytic sarcomas (Table 2). Also, *Mdm2*^{SNP309G/G} mice treated with 1Gy IR had significantly increased ($p<0.0001$) tumor multiplicity compared to non-irradiated genotypes and irradiated *Mdm2*^{SNP309T/T} mice (Figure 11). Only irradiated *Mdm2*^{SNP309G/G} mice had three or more tumors per mouse. These data show low-dose ionizing radiation exacerbates tumor development in *Mdm2*^{SNP309G/G} mice compared to *Mdm2*^{SNP309T/T} mice.

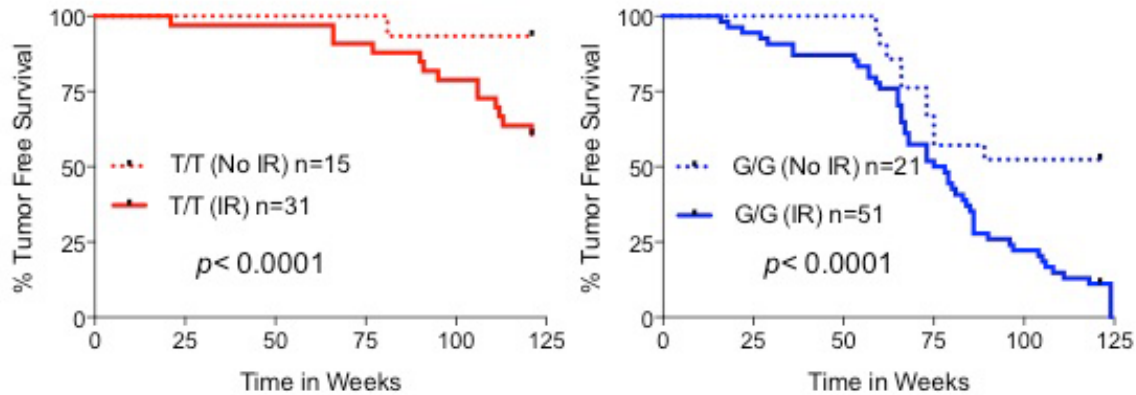


Figure 7. Tumor-free survival curves of *Mdm2*^{SNP309} mice comparing non-irradiated and irradiated mice. Numbers reflect mouse numbers in the cohorts. The parentheses represent the environmental exposure. The only group that reached median tumor-free survival is the G/G IR with 74 weeks. The statistical differences in the curves were measured using a Log-rank test. IR, ionizing radiation; *Mdm2*^{SNP309T/T}, T/T; *Mdm2*^{SNP309G/G}, G/G.

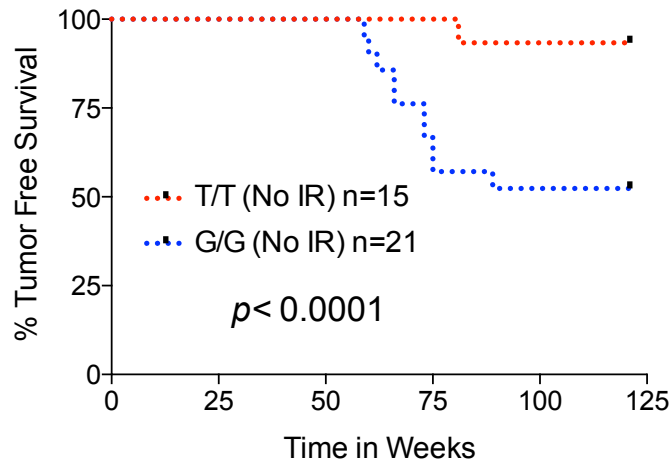


Figure 8. Tumor-free survival of non-irradiated $Mdm2^{SNP309}$ mice. Numbers reflect mouse numbers in the cohorts and the parentheses represent the environmental exposure. No group reached median tumor-free survival. The statistical differences in the curves were measured using a Log-rank test. IR, ionizing radiation; $Mdm2^{SNP309T/T}$, T/T; $Mdm2^{SNP309G/G}$, G/G.

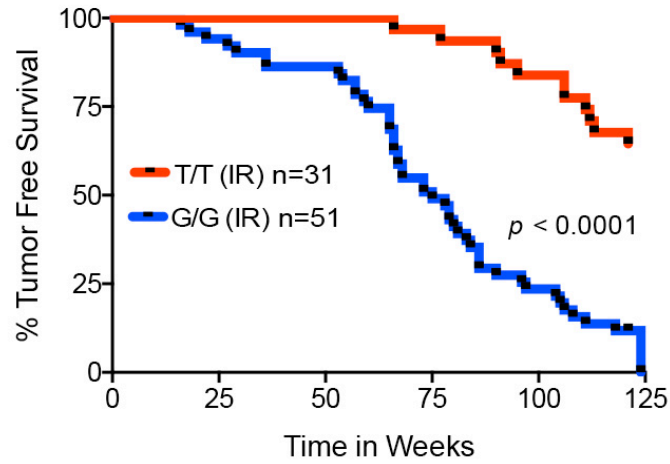


Figure 9. Tumor-free survival of gamma-irradiated *Mdm2*^{SNP309} mice. Numbers reflect mouse numbers in the cohorts. The parentheses represent the environmental exposure. The G/G IR group reached median tumor-free survival with 74 weeks. The statistical differences in the curves were measured using a Log-rank test. IR, ionizing radiation; *Mdm2*^{SNP309T/T}, T/T; *Mdm2*^{SNP309G/G}, G/G.

Tumor Type	<i>Mdm2</i> ^{SNP309T/T} (1/15 =6%)	<i>Mdm2</i> ^{SNP309G/G} (11/21 =52%)
Lymphoma		2
Osteosarcoma		9
Hepatocellular	1	1
Histiocytic Sarcoma		1
Total tumors per genotype	1	13

Table 1. Tumor spectrum in non-irradiated *Mdm2*^{SNP309} mice. n represents number of mice that presented with tumors. The numbers in parentheses represent percent of mice presenting tumors per genotype. The bold numbers represent total tumors per genotype.

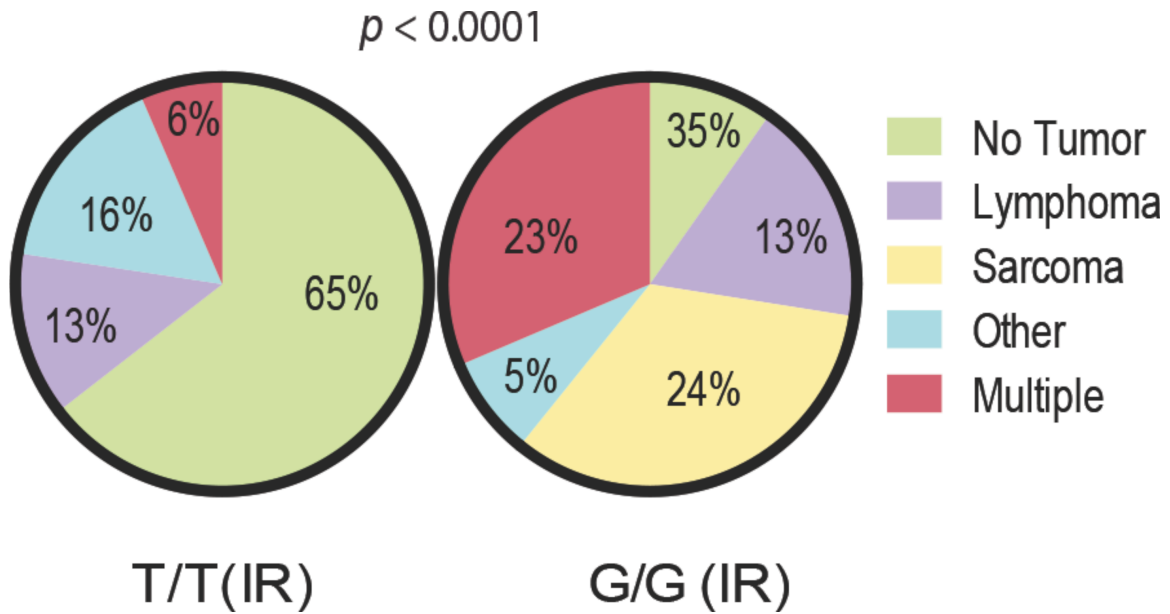


Figure 10. Tumor incidence in gamma-irradiated *Mdm2*^{SNP309} mice. The pie charts represent the comparison between tumor spectrum of T/T and G/G groups treated with gamma radiation. The comparisons were calculated using Fishers test. IR, ionizing radiation; *Mdm2*^{SNP309T/T}, T/T; *Mdm2*^{SNP309G/G}, G/G.

Tumor Type	<i>Mdm2</i> ^{SNP309T/T} (11/31 =35%)	<i>Mdm2</i> ^{SNP309G/G} (46/51 =90%)
Lymphoma	4	17
NOS		2
Rhabdomyosarcoma		1
Hemangiosarcoma		3
Osteosarcoma	2	25
Medulloblastoma		1
Glioblastoma		1
Neuroblastoma		1
Adenoma	2	3
Alveolar carcinoma		2
Hepatocellular carcinoma	3	4
Mammary carcinoma		2
Renal tubule		1
Squamous cell carcinoma		1
Histiocytic sarcoma	1	4
Germ cell tumor	1	2
Total tumors	13	70

Table 2. Tumor spectrum of *Mdm2*^{SNP309} C57BL/6 mice after 1Gy IR. n represents number of mice that presented with tumors. The numbers in parentheses represent percent of mice presenting tumors per genotype. The bold numbers represent total tumors per genotype.

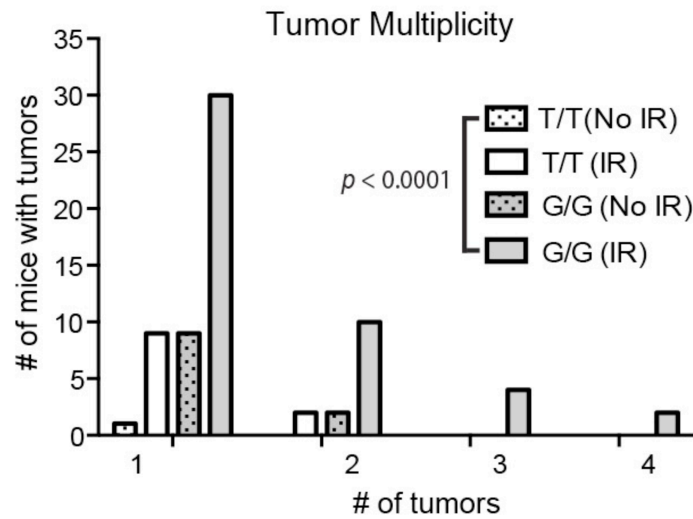


Figure 11. Tumor multiplicity of *Mdm2*^{SNP309} C57BL/6 mice cohort. The y-axis represents the number of mice with tumors. The x-axis represents number of tumors. The comparison was conducted with Fishers exact test.

Low-dose ionizing radiation exacerbates lymphoma development in *Mdm2*^{SNP309G/G} mice compared to *Mdm2*^{SNP309T/T} mice

I further characterized the lymphoma phenotype due to its high penetrance (Figure 12) where lymphoma-free survival shows irradiated *Mdm2*^{SNP309G/G} mice developed lymphomas significantly faster ($p < 0.0001$) compared to *Mdm2*^{SNP309T/T} mice. To determine the lymphoma phenotype, I performed immunohistochemistry (IHC) with CD3 (T cell marker) and B220 antibodies (B-cell marker) and observed that lymphomas from *Mdm2*^{SNP309G/G} mice were either T-cell or B-cell lymphomas (Figure 13), with the majority being of T cell origin (66%).

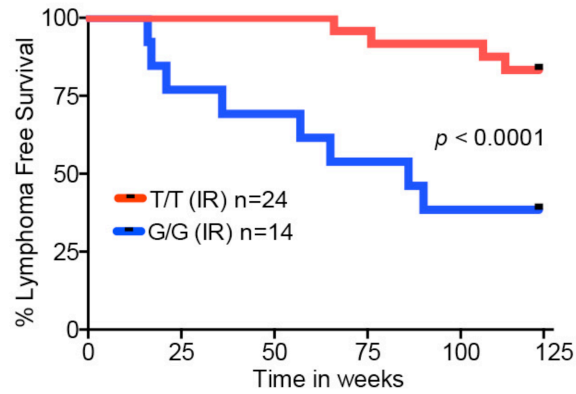


Figure 12. Lymphoma-free survival of gamma-irradiated *Mdm2*^{SNP309} mice. Numbers reflect mouse numbers in the cohorts. The parentheses represent the environmental exposure. The median lymphoma-free survival of G/G IR group was 80 weeks. The statistical differences in the curves were measured using a Log-rank test. IR, ionizing radiation; *Mdm2*^{SNP309T/T}, T/T; *Mdm2*^{SNP309G/G}, G/G.

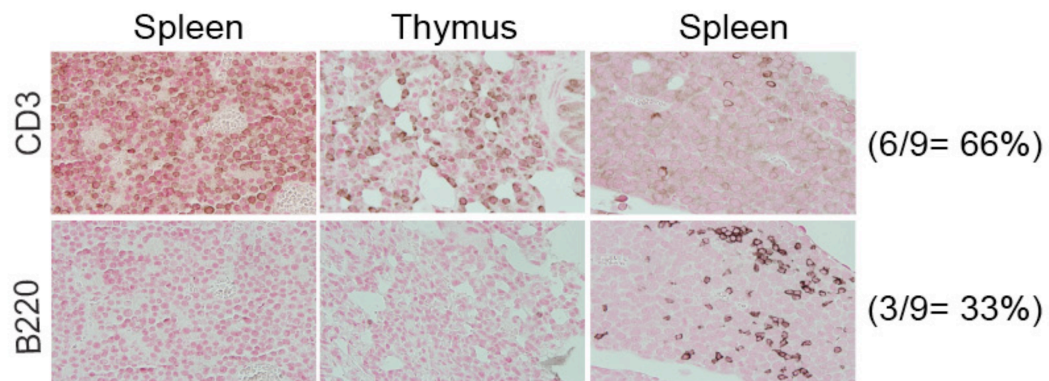


Figure 13. Lymphomas in $Mdm2^{SNP309G/G}$ mice exhibit either T-cell or B-cell cell-type. The tissues were necropsied from $Mdm2^{SNP309G/G}$ mice. Dr. Adel El-Naggar identified the samples as lymphomas. The numbers in parentheses represent the percentage of tissues that stain positive for that particular antibody.

Interim summary

These experiments demonstrate that the *Mdm2*^{SNP309G} allele impacts p53 activity. Experiments show that lymphatic tissues harvested from *Mdm2*^{SNP309G/G} mice express higher *Mdm2* levels and exhibit less apoptotic activity compared to *Mdm2*^{SNP309T/T} tissues. Furthermore, *Mdm2*^{SNP309G/G} mice show exacerbated spontaneous tumor development after low-dose IR compared to the *Mdm2*^{SNP309T/T} mice. Finally, *Mdm2*^{SNP309G/G} mice are more prone to lymphomas of either T-cell or B-cell cell-type origin compared to the *Mdm2*^{SNP309T/T} mice.

The effects of low-dose IR in lymphatic tissues show a delay in apoptosis in spleen and thymi of *Mdm2*^{SNP309G/G} mice compared to *Mdm2*^{SNP309T/T} tissues. Previous studies show that delayed apoptotic response to gamma irradiation correlated with increased cancer risk [135], providing some insight into lymphoma susceptibility in our model.

Investigating the influence of Ultraviolet radiation on *Mdm2*^{SNP309} skin cancer risk

Rational

Previous research conclusively showed that the *SNP309G* allele is the ‘at risk’ allele for tumor risk [107, 119]. My previous experiments show *Mdm2*^{SNP309G/G} mice exhibit increased cancer risk after exposure to low-dose ionizing radiation compared to *Mdm2*^{SNP309T/T} mice. To further examine the influence of other environmental factors on the *SNP309G* allele and cancer risk, we investigated the influence of ultraviolet radiation on *Mdm2*^{SNP309} mice and skin cancer. Ultraviolet (UV) radiation is the primary environmental cause of skin cancer in humans [136]. UVB causes pro-mutagenic DNA lesions that result in bulky DNA adducts composed mostly of thymine dimers and 6,4-photoproducts [137]. Nucleotide excision repair (NER) removes DNA damage induced by UVB by recognizing damage site and removes short single-stranded DNA segment that contains the lesion [138]. Furthermore, exposure to UVB radiation induces intracellular reactive oxygen species, which elicit a robust p53 response [139, 140] and leads to skin cancer development [141]. The C57BL/6 strain mouse is resistant to skin tumors [142], and thus is not an adequate model. However, the FVB mouse strain is susceptible to insult-induced skin tumorigenesis and has been characterized as a model for studying progressive squamous cell carcinoma [143]. Thus, we hypothesized that UVB radiation would exacerbate tumor development in *Mdm2*^{SNP309G/G} mice compared to *Mdm2*^{SNP309T/T} mice in an FVB background strain. To this end, we generated cohorts of *Mdm2*^{SNP309T/T} and *Mdm2*^{SNP309G/G} mice in an FVB background strain (+99%), treated them with UVB radiation, and followed them for tumor formation.

Note: section 2.2 was conducted in a collaborative effort with Dr. David G. Johnson's laboratory.

Ultraviolet radiation preferably attenuates p53 activity in epidermis tissue from *Mdm2*^{SNP309T/T} mice compared to *Mdm2*^{SNP309G/G} mice

I first characterized the effect of ultraviolet radiation (UVB) on *Mdm2* levels and p53 activity in keratinocytes of *Mdm2*^{SNP309T/T} and *Mdm2*^{SNP309G/G} mice in an FBV strain background. To test the effects of UVB on *Mdm2* in keratinocytes, primary keratinocytes were treated with a single dose of UVB (100mJ/cm²) and RNA was isolated. Primary keratinocytes were isolated from *Mdm2*^{SNP309G/G} and *Mdm2*^{SNP309T/T} mouse epidermis and RNA was extracted from the cells. In contrast to studies in the spleen (Figure 3), primary keratinocytes from *Mdm2*^{SNP309T/T} mice showed relatively higher *Mdm2* basal levels as compared to keratinocytes from *Mdm2*^{SNP309G/G} mice (Figure 14). Consistent with the non-treated samples, keratinocytes isolated from *Mdm2*^{SNP309T/T} mice showed greater than two-fold higher *Mdm2* levels ($p=0.001$) 24 hours post UVB treatment compared to *Mdm2*^{SNP309G/G} keratinocytes (Figure 14).

To test the effects of UVB on p53 activity in skin tissue, the epidermis from 6-week old *Mdm2*^{SNP309G/G} and *Mdm2*^{SNP309T/T} mice were treated with a single dose of UVB (100mJ/cm²), a dose previously shown to activate acute p53 response in skin tissue [144], and analyzed for p21 protein expression to evaluate p53 activity. Consistent with the elevated *Mdm2* expression levels in keratinocytes from *Mdm2*^{SNP309T/T} compared to *Mdm2*^{SNP309G/G} mice after UVB treatment, *Mdm2*^{SNP309G/G} keratinocytes displayed a significantly higher number of cells staining positive for p21 ($p=0.019$) compared to

Mdm2^{SNP309T/T} keratinocytes (Figure 15). These data show that *Mdm2* expression is greater in skin from *Mdm2*^{SNP309T/T} mice compared to *Mdm2*^{SNP309G/G} mice and that UVB irradiation elevates *Mdm2* levels more in skin tissue of *Mdm2*^{SNP309T/T} mice compared to *Mdm2*^{SNP309G/G} mice with a concomitant attenuated p53 response.

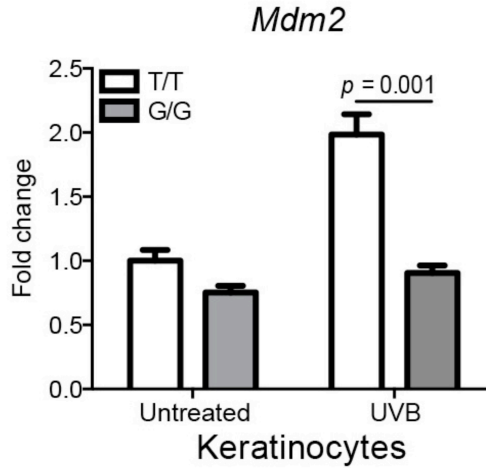


Figure 14. *Mdm2* expression in *Mdm2*^{SNP309} keratinocytes 24h post UV radiation. RT-qPCR analysis of *Mdm2* expression in keratinocytes from *Mdm2*^{SNP309T/T} and *Mdm2*^{SNP309G/G} mice 24 hours post UV radiation (100mJ/cm²). Three mice per genotype were analyzed. The average expression of untreated (T/T) keratinocytes was normalized to 1 for comparison. Keratin 14 expression (housekeeping gene) was used as internal control. UVB, ultraviolet radiation; *Mdm2*^{SNP309T/T}, T/T; *Mdm2*^{SNP309G/G}, G/G.

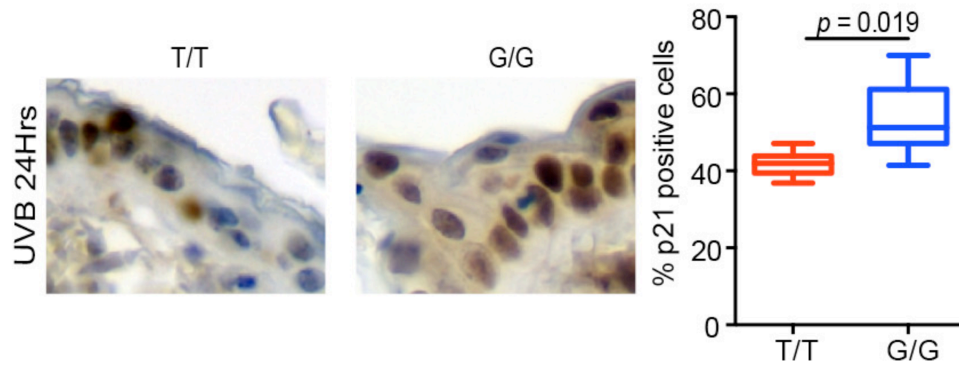


Figure 15. Expression analysis of p53 targets in *Mdm2*^{SNP309} skin tissues 24h post UVB. Protein expression analysis of p21 in skin tissues of *Mdm2*^{SNP309T/T} and *Mdm2*^{SNP309G/G} mice 24 hours post UV radiation (100mJ/cm²). Three mice per genotype were analyzed. The graph represents the percent of cells positive for p21 protein expression. UVB, ultraviolet radiation; *Mdm2*^{SNP309T/T}, T/T; *Mdm2*^{SNP309G/G}, G/G.

Ultraviolet radiation exacerbates squamous cell carcinoma development in *Mdm2*^{SNP309T/T} mice compared to *Mdm2*^{SNP309G/G} mice

To examine the long-term effects of UVB exposure on skin cancer risk, a cohort of *Mdm2*^{SNP309G/G} and *Mdm2*^{SNP309T/T} mice in an FVB background was generated and treated with an established UVB regimen [144] (UVB radiation three times per week for 30 weeks) and monitored for spontaneous tumor development. The cohort was observed for 40 weeks because most mice, independent of genotype, acquire squamous cell carcinoma within this time frame. Tumor-free survival analysis of UVB-treated mice also showed that *Mdm2*^{SNP309T/T} mice exhibit significantly sooner onset to UVB-induced squamous cell carcinoma than *Mdm2*^{SNP309G/G} mice ($p < 0.0001$) (Figure 16) with a median survival of 28 weeks compared to 36 weeks. Non-UV treated FVB mice did not develop skin tumors [145]. Further assessment of the tumor-free survival stratified by gender show that male *Mdm2*^{SNP309G/G} mice were significantly delayed in tumor development ($p < 0.0001$) compared to the other groups (Figure 16). Moreover, *Mdm2*^{SNP309G/G} female mice develop UVB-induced skin SCC at a later age compared to female *Mdm2*^{SNP309T/T} mice. The data showed that the long-termed effects of UVB treatment increased death of *Mdm2*^{SNP309T/T} mice through squamous cell carcinoma development compared to *Mdm2*^{SNP309G/G} mice.

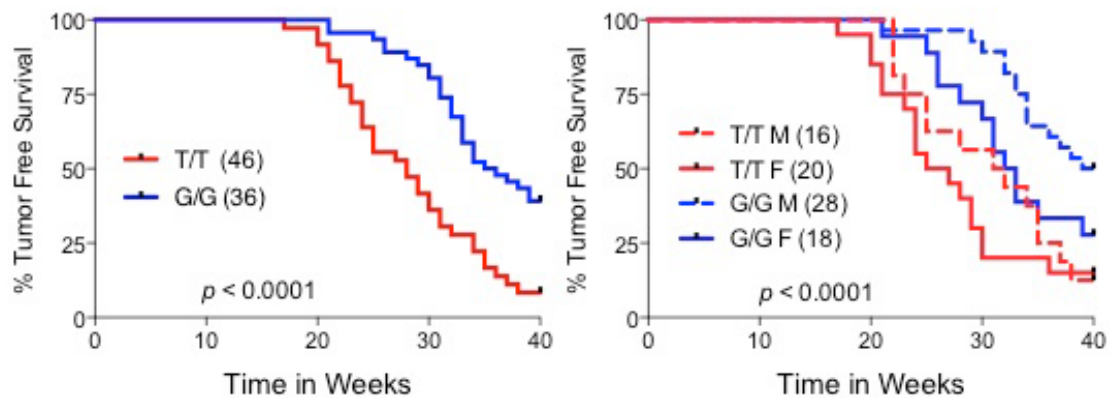


Figure 16. Tumor-free survival of UVB-irradiated *SNP309* mice. Numbers reflect mouse numbers in the cohorts. The parentheses represent the environmental exposure. The G/G UVB group reached median tumor-free survival of 36 weeks compared to T/T group, which reach 28 weeks. Tumor free survival by gender shows that G/G males are more resistant to tumors compared to the rest of the groups ($p < 0.0001$). The statistical differences in the curves were measured using a Log-rank test. UVB, ultraviolet radiation; *Mdm2*^{SNP309T/T}, T/T; *Mdm2*^{SNP309G/G}, G/G; M= male, F= female.

Ultraviolet radiation increases *Mdm2* expression in a tissue-dependent manner in *Mdm2*^{SNP309} mice

UV treatment led to a dampened p53 response and shorter tumor latency in *Mdm2*^{SNP309T/T} mice compared to *Mdm2*^{SNP309G/G} mice in an FVB mouse background strain. These data are in contrast to the *Mdm2*^{SNP309} IR treatment results, which were conducted in a C57BL/6 mouse strain background. These data suggest that either the type of DNA damage, cell type, or mouse strain account for the differences in tumorigenesis. Previous data show that fibroblasts harvested from *Mdm2*^{SNP309T/T} and *Mdm2*^{SNP309G/G} mice in C57BL/6 strain background show higher basal *Mdm2* levels in *Mdm2*^{SNP309G/G} than in *Mdm2*^{SNP309T/T} genotype [119]. Therefore, we hypothesized that fibroblasts harvested from *Mdm2*^{SNP309G/G} mice in FVB strain would exhibit higher *Mdm2* levels compared to *Mdm2*^{SNP309T/T} mice after UVB treatment. Thus, primary fibroblasts from *Mdm2*^{SNP309T/T} and *Mdm2*^{SNP309G/G} FVB mice were harvested were treated with a single dose of UVB (100mJ/cm²) and prepared for RNA isolation. The results show 1.9-fold higher ($p=0.001$) increase in *Mdm2* expression 24 hours post UVB treatment in *Mdm2*^{SNP309G/G} compared to *Mdm2*^{SNP309T/T} fibroblasts (Figure 17), suggesting that the contrasting differences in *Mdm2* levels in fibroblasts were not strain-dependent.

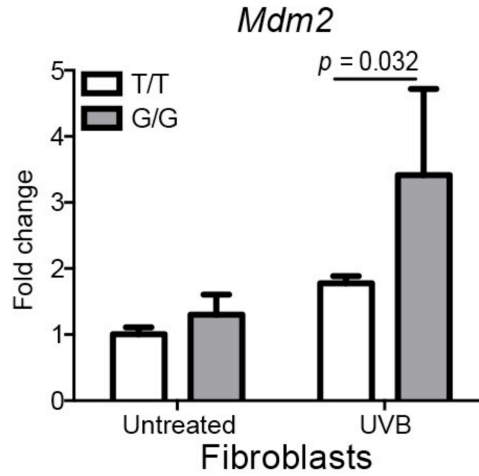


Figure 17. *Mdm2* expression in *Mdm2*^{SNP309} primary fibroblasts cells from FVB mice 24h post UV radiation. RT-qPCR analysis of *Mdm2* expression in the fibroblasts from *Mdm2*^{SNP309T/T} and *Mdm2*^{SNP309G/G} mice 24 hours post UV radiation (100mJ/cm²). Three mice per genotype were analyzed. The average expression of untreated (T/T) fibroblasts was normalized to 1 for comparison. GAPDH expression (housekeeping gene) was used as internal control. UVB, ultraviolet radiation; *Mdm2*^{SNP309T/T}, T/T; *Mdm2*^{SNP309G/G}, G/G.

Epidermal tissue from *Mdm2*^{SNP309T/T} mice exhibit higher *Mdm2* expression independent of insult compared to *Mdm2*^{SNP309G/G} mice

Benzo(a)pyrene (B(a)P) is a tobacco-related carcinogen that causes DNA damage [146]. To determine if the differences in skin tumor onset are limited to UVB insult, we next investigated the effects of B(a)P on p53 activity in the skin of our mice. The epidermis of *Mdm2*^{SNP309G/G} and *Mdm2*^{SNP309T/T} mice was treated with either acetone (control) or B(a)P, and total RNA was isolated 24-hour post treatment. *Mdm2* mRNA levels were higher in *Mdm2*^{SNP309T/T} mice compared to *Mdm2*^{SNP309G/G} mice after B(a)P treatment. However, the differences were not statistically significant (Figure 18).

To examine tumor risk following B(a)P exposure, we treated *Mdm2*^{SNP309G/G} and *Mdm2*^{SNP309T/T} mice to an established regimen of 317 nmol of B(a)P once a week for 30 weeks [146] and monitored mice for spontaneous tumor formation. Tumor-free survival showed that B(a)P treated *Mdm2*^{SNP309T/T} mice were more susceptible than *Mdm2*^{SNP309G/G} mice ($p<0.0001$) (Figure 19) with a median survival of 22 weeks compared to 25 weeks, respectively. Further assessment of the tumor-free survival data showed that the difference was primarily due to gender (Figure 20). Tumor development in male *Mdm2*^{SNP309G/G} mice was significantly delayed ($p<0.0001$) compared to the other groups. We, therefore, revisited the *Mdm2* expression levels in the epidermis of *Mdm2*^{SNP309G/G} and *Mdm2*^{SNP309T/T} male mice. Similarly, *Mdm2* mRNA levels were significantly lower ($p=0.03$) in the epidermis of male *Mdm2*^{SNP309G/G} mice compared to male *Mdm2*^{SNP309T/T} mice 24-hour post B(a)P treatment, but there were no significant differences between female mice (Figure 21). Moreover, epidermal keratinocytes in skin samples from male

Mdm2^{SNP309G/G} mice displayed a significantly higher number of cells staining positive for p21 ($p=0.04$) as compared to *Mdm2*^{SNP309T/T} keratinocytes after B(a)P treatment (Figure 22). Altogether, the data show that keratinocytes from male *Mdm2*^{SNP309G/G} mice exhibited significantly lower *Mdm2* expression and increased p53 activity in *Mdm2*^{SNP309G/G} mice compared to *Mdm2*^{SNP309T/T} mice in response to B(a)P insult. Thus, *Mdm2*^{SNP309G/G} mice, particularly males, are more resistant to developing skin SCC in response to B(a)P treatment.

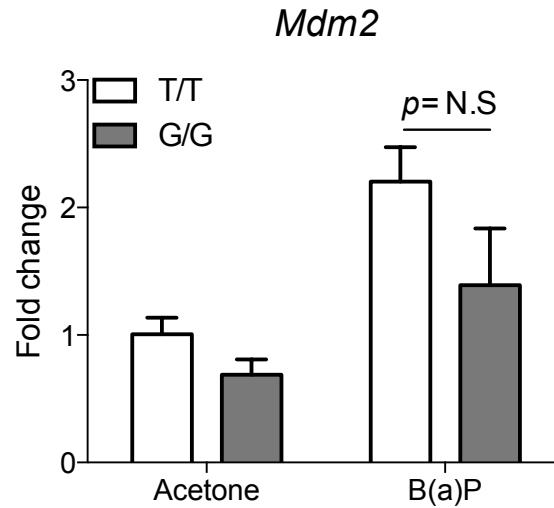


Figure 18. *Mdm2* expression in *Mdm2*^{SNP309} epidermis tissues 24h post B(a)P treatment. RT-qPCR analysis of *Mdm2* expression in epidermis tissues from *Mdm2*^{SNP309T/T} and *Mdm2*^{SNP309G/G} mice 24 hours post B(a)P treatment. Six mice per genotype represent the analysis. The average expression of control (Acetone) T/T epidermis was normalized to 1 for comparison. Keratin 14 expression (housekeeping gene) was used as internal control. B(a)P, Benzo(a)pyrene; *Mdm2*^{SNP309T/T}, T/T; *Mdm2*^{SNP309G/G}, G/G; N.S= not significant.

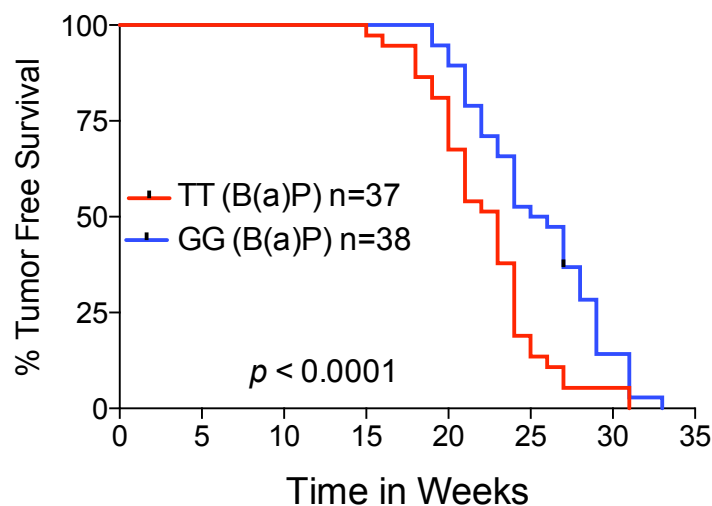


Figure 19. Tumor-free survival of B(a)P treated *Mdm2*^{SNP309} mice. Numbers reflect mouse numbers in the cohorts. The parentheses represent the environmental exposure. The G/G B(a)P group reached median tumor-free survival of 25 weeks compared to T/T group, which reached 22 weeks. The statistical differences in the curves were measured using a Log-rank test. B(a)P, Benzo(a)pyrene; *Mdm2*^{SNP309T/T}, T/T; *Mdm2*^{SNP309G/G}, G/G.

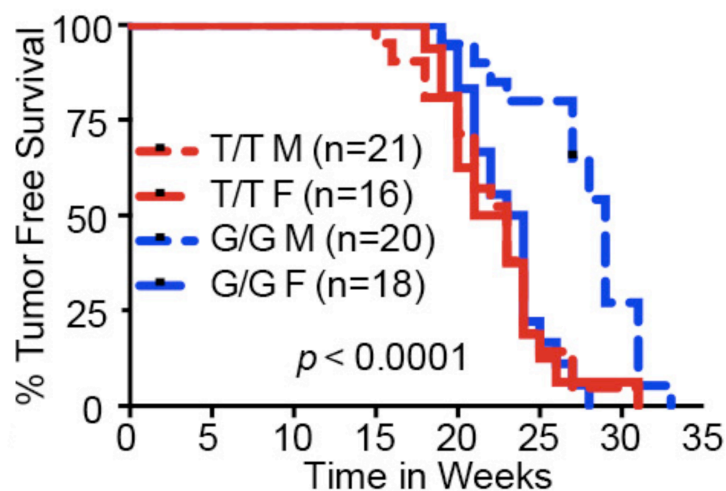


Figure 20. Tumor-free survival of B(a)P treated $Mdm2^{SNP309}$ mice separated by gender. Numbers in parentheses reflect mouse numbers in the cohorts. The statistical differences in the curves were measured using a Log-rank test. B(a)P, Benzo(a)pyrene; $Mdm2^{SNP309T/T}$, T/T; $Mdm2^{SNP309G/G}$, G/G; M= male, F= female.

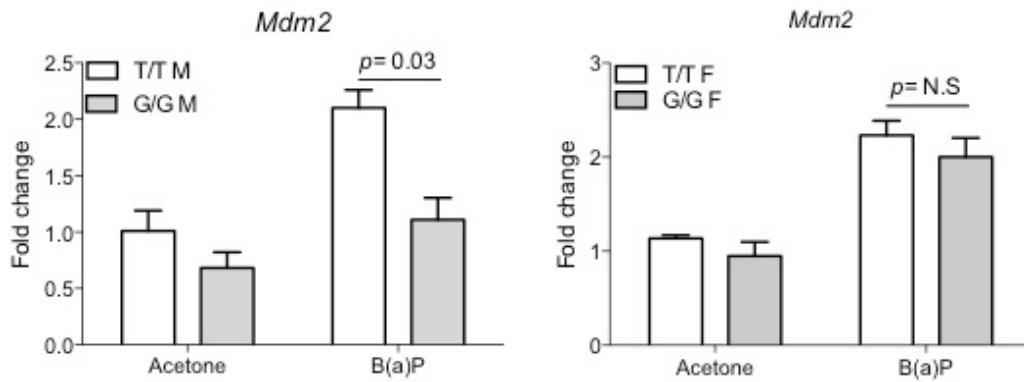


Figure 21. *Mdm2* expression in epidermis tissues of male and female *Mdm2*^{SNP309} mice 24h post B(a)P treatment. RT-qPCR analysis of *Mdm2* expression in the epidermis from male and female *Mdm2*^{SNP309T/T} and *Mdm2*^{SNP309G/G} mice 24 hours post B(a)P treatment. Three mice per genotype represent the analyses. The average expression of control (Acetone) T/T epidermis was normalized to 1 for comparison. Keratin 14 expression (housekeeping gene) was used as internal control. B(a)P, Benzo(a)pyrene; *Mdm2*^{SNP309T/T}, T/T; *Mdm2*^{SNP309G/G}, G/G; M= male, F= female; N.S= not significant.

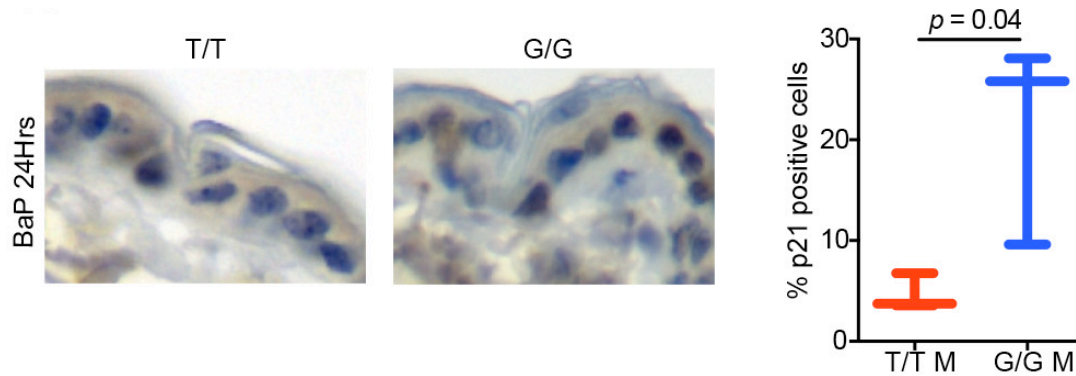


Figure 22. Expression analysis of p53 targets in male *SNP309* skin tissues 24h post B(a)P treatment. Protein expression analysis of p21 by IHC in skin tissues from male *Mdm2*^{SNP309T/T} and *Mdm2*^{SNP309G/G} mice 24 hours post B(a)P treatment. Three mice per genotype represent the analysis, and the number of positive cells per field of view was counted in three sections per mouse. The graph represents the percent of cells positive for p21 protein expression. B(a)P, Benzo(a)pyrene; *Mdm2*^{SNP309T/T}, T/T; *Mdm2*^{SNP309G/G}, G/G; M= male.

Interim summary

The influence of UV exposure led to a dampened p53 response and shorter tumor latency in *Mdm2*^{SNP309T/T} mice compared to *Mdm2*^{SNP309G/G} mice, in contrast to IR treatment. The evaluation of *the Mdm2* expression in different tissues (keratinocytes and fibroblasts) after UVB treatment suggests that the cell-type accounts for the differences in tumorigenesis. Furthermore, B(a)P treatment in the skin of *SNP309* mice exhibit shorter tumor latency in *Mdm2*^{SNP309T/T} mice compared to *Mdm2*^{SNP309G/G} mice, consistent with UVB experiment. Thus exposure to skin insult predisposes *Mdm2*^{SNP309T/T} mice to SCC compared to *Mdm2*^{SNP309G/G} mice.

Investigating the role of the *SNP309G* allele in *Mdm2* regulation in a tissue-dependent manner

Thus far, the data suggest that the influence of environmental factors on *SNP309* cancer risk in mice is cell-type-dependent. Therefore, I hypothesized that the *Mdm2* regulation in *SNP309* mice occurs in a tissue-dependent manner. To this end, I harvested tissues from *SNP309* mice and evaluated the *Mdm2* basal expression in different tissues. Furthermore, I employed *in silico* analysis to examine transcription factor candidates that may differentially bind to the *MDM2* P2 promoter in a tissue-specific manner. Finally, I utilized tissues from *SNP309* mice to investigate the possible *SNP309*-dependent mechanism(s) of *Mdm2* regulation in different tissues.

***Mdm2* expression is tissue-dependent in *Mdm2 SNP309* mice**

To address the opposite differences in vulnerability to cancer risk after exposure to environmental factors, I evaluated the *Mdm2* basal expression in different tissues harvested from *Mdm2*^{*SNP309G/G*} and *Mdm2*^{*SNP309T/T*} mice in a C57BL/6 background. *Mdm2* basal levels vary in different tissues in an SNP-dependent manner (Figure 23). *Mdm2* mRNA levels in the thymus (the origin of T-cell lymphomas) of *Mdm2*^{*SNP309G/G*} mice are statistically higher ($p=0.04$) than in *Mdm2*^{*SNP309T/T*} mice. Conversely, keratinocytes, the cell of origin for SCC, in *Mdm2*^{*SNP309T/T*} mice exhibit significantly higher *Mdm2* mRNA levels ($p=0.001$) than keratinocytes in *Mdm2*^{*SNP309G/G*} mice. Similarly, epidermis, a source of keratinocytes, isolated from *Mdm2*^{*SNP309T/T*} FVB mice show significantly higher *Mdm2* basal levels ($p=0.04$) compared to *Mdm2*^{*SNP309G/G*} FVB mice (Figure 24). Thus,

keratinocytes from *Mdm2*^{SNP309G/G} mice exhibit lower *Mdm2* basal levels compared to keratinocytes from *Mdm2*^{SNP309T/T} mice independent of mouse strain. One other tissue showed significant differences in *Mdm2* levels; the heart tissue exhibited significantly higher *Mdm2* mRNA levels ($p=0.006$) in *Mdm2*^{SNP309G/G} mice than in *Mdm2*^{SNP309T/T} mice (Figure 23). Further investigation showed that other tissues exhibited significant differences in *Mdm2* basal levels when evaluated by gender (Figure 25).

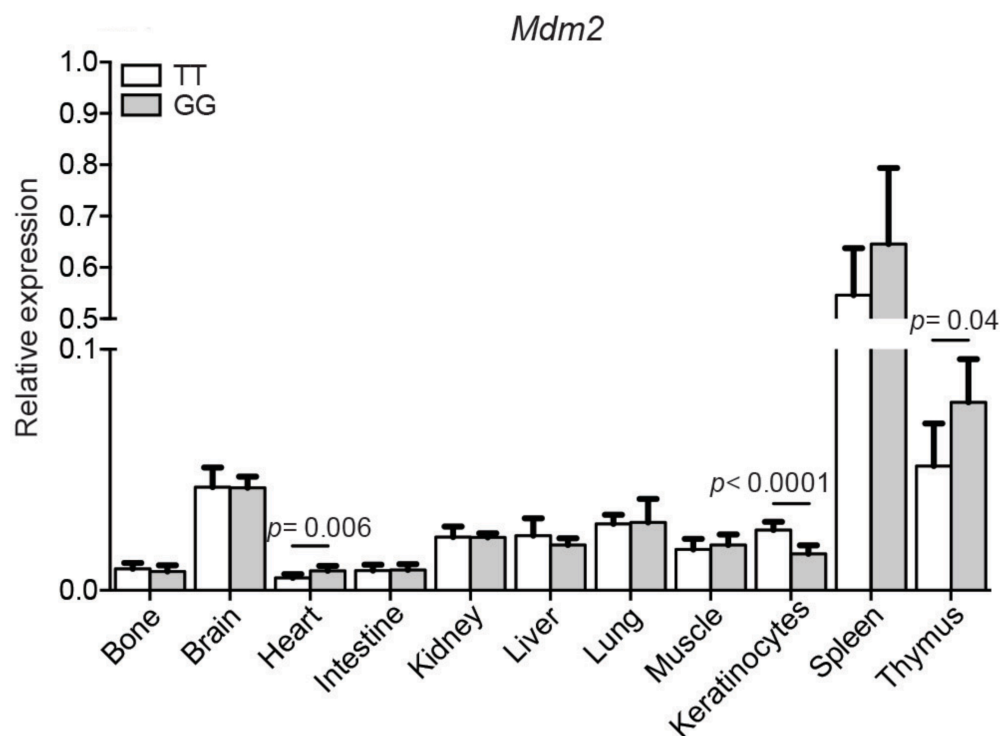


Figure 23. *Mdm2* basal expression in tissues of *SNP309* mice in C57BL/6 strain. RT-qPCR analysis of *Mdm2* expression in different tissues from *Mdm2*^{SNP309T/T} and *Mdm2*^{SNP309G/G} mice. Eight mice per genotype in each tissue type were analyzed. *RplpO* expression (housekeeping gene) was used as internal control. *Mdm2*^{SNP309T/T}, T/T; *Mdm2*^{SNP309G/G}, G/G.

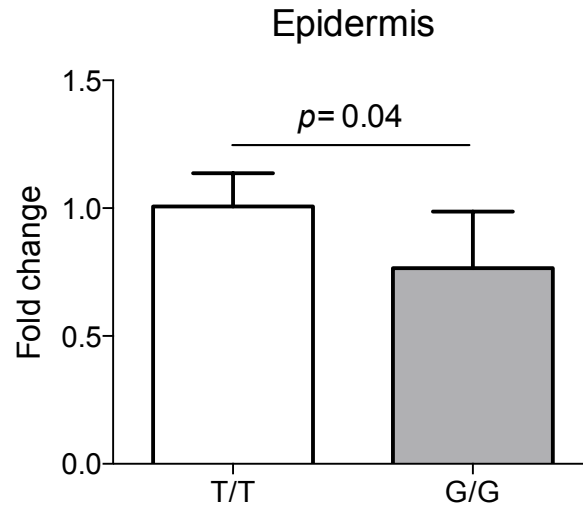


Figure 24. *Mdm2* basal expression in epidermis of *SNP309* mice in FVB strain. RT-qPCR analysis of *Mdm2* expression in the epidermis from *Mdm2*^{*SNP309T/T*} and *Mdm2*^{*SNP309G/G*} mice. Six mice per genotype were analyzed. The average expression of T/T epidermis was normalized to 1 for comparison. Keratin 14 expression (housekeeping gene) was used as internal control. *Mdm2*^{*SNP309T/T*}, T/T; *Mdm2*^{*SNP309G/G*}, G/G.

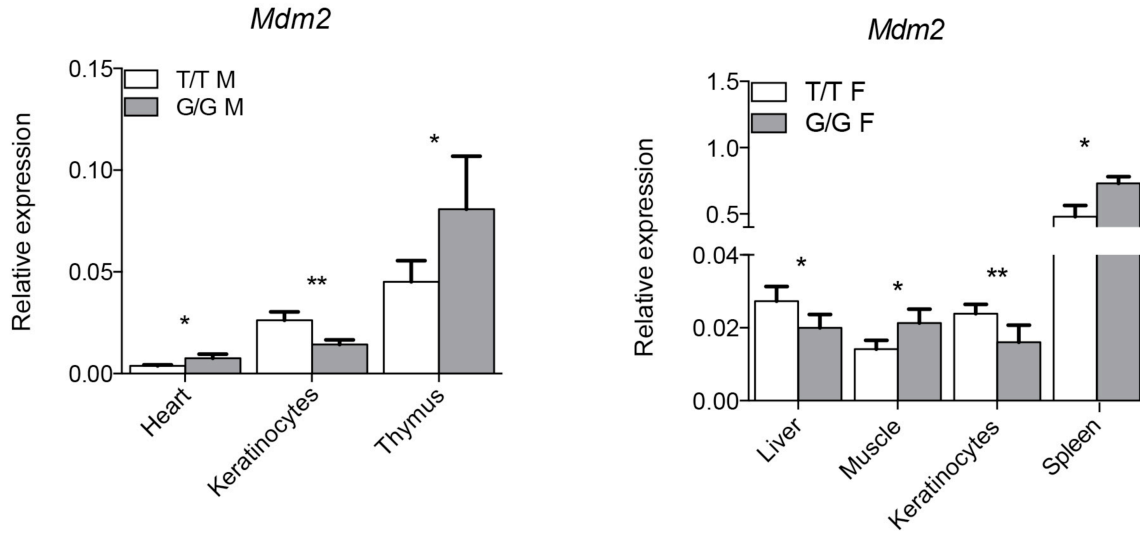


Figure 25. *Mdm2* basal expression in *SNP309* mouse by gender. RT-qPCR analysis of *Mdm2* expression in the different tissues from *Mdm2*^{SNP309T/T} and *Mdm2*^{SNP309G/G} mice separated by gender. Four mice per genotype (per gender) in each tissue type were analyzed. The average expression of T/T tissues was normalized to 1 for comparison. *RplpO* expression (housekeeping gene) was used as internal control. *Mdm2*^{SNP309T/T}, T/T; *Mdm2*^{SNP309G/G}, G/G; M= male, F= female; * = $p < 0.01$, ** = $p < 0.001$.

The identification of E2F family members as transcriptional regulators of the *Mdm2* gene

To investigate the mechanism by which the *SNP309* alleles regulate *Mdm2* expression in a tissue-specific manner, we first interrogated potential transcription factor binding to the *SNP309* allele. Analyses of the ENCODE ChIP-seq database [147] in genome browser (<https://genome.ucsc.edu>) showed that transcriptional repressors E2F4 and E2F6 were candidates because of their binding proximity to *SNP309* (Figures 26, 27). Additionally, previous studies associated these repressors as key regulators of keratinocyte proliferation [148]. The cell lines utilized in the ENCODE ChIP-seq experiments for E2F4 and E2F6 were MCF10A and K562, respectively. Sequence analysis of these cell lines showed that MCF10A cells harbor a homozygous *SNP309T* genotype and K562 cells harbor a *SNP309T/G* genotype (Figure 28).

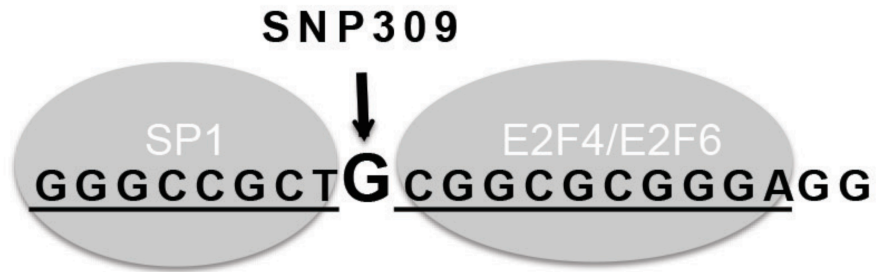


Figure 26. Predicted SP1 & E2F binding sites in the *MDM2* P2 promoter proximal to *SNP309* site. Analyses of the ENCODE ChIP-seq database was conducted through genome browser.

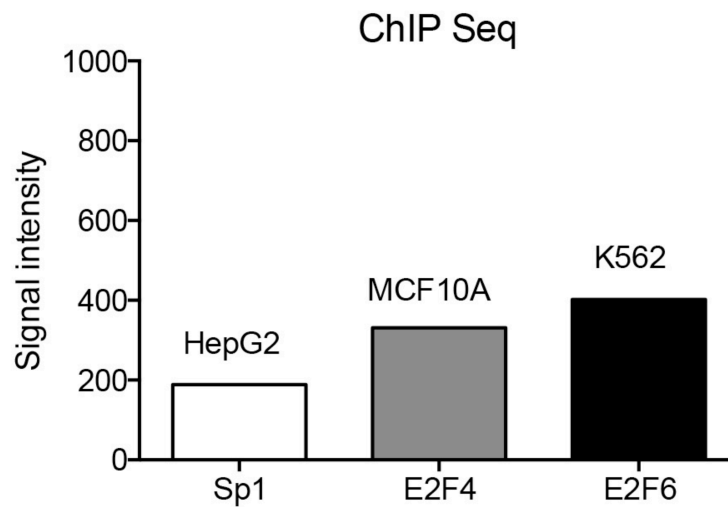


Figure 27. ENCODE ChIP-seq transcription factor binding analysis proximal to position 309 in the MDM2-P2 promoter. Intensity was calculated of possible 1000 units.

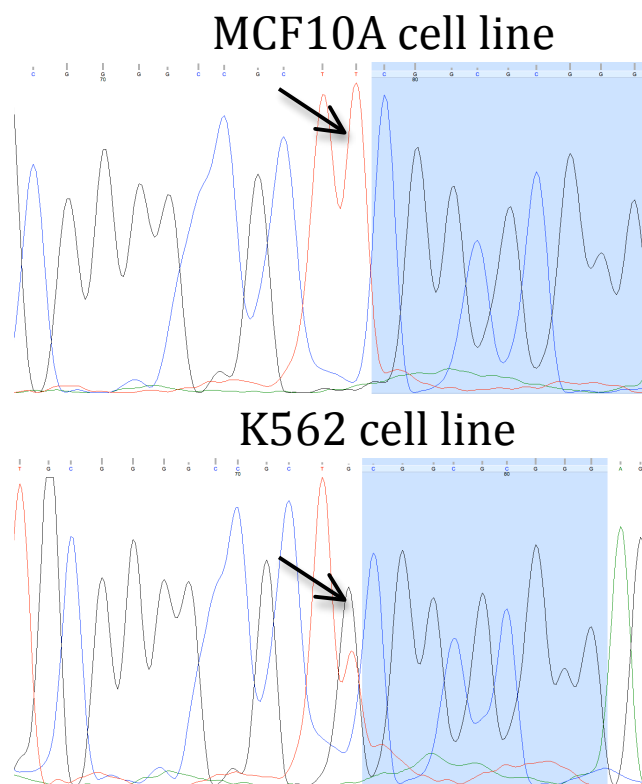


Figure 28. Sequencing MCF10A and K562 cell lines for the *Mdm2* SNP309. The analysis was conducted through Sanger sequencing. MCF10A cell line harbors *MDM2* SNP309T/T and K562 *MDM2* SNP309 T/G.

Transcriptional repressor E2F6 negatively regulates *Mdm2* expression in *SNP309G* cells but not in *SNP309T* cells

To examine if E2F4 and E2F6 regulate *Mdm2* expression in an *SNP309* allele-dependent manner, we generated MEFs from *Mdm2*^{*SNP309G/G*} and *Mdm2*^{*SNP309T/T*} C57BL/6 mice and transfected them with plasmids expressing GFP and either E2F4, E2F6, or SP1, a transcriptional activator that increases *Mdm2* expression in *Mdm2*^{*SNP309G/G*} cells. Cells were sorted based on GFP expression, and GFP positive cells were analyzed via RT-qPCR. As expected, sorted cells expressing GFP and Sp1 preferentially increased *Mdm2* expression in *SNP309G* MEFs ($p < 0.001$) (Figure 29). E2F4 transfection increased *Mdm2* expression slightly in *SNP309T* cells, but there were no significant differences between genotypes (Figure 30). E2F6 transfection statistically repressed transcription of *Mdm2* in *SNP309G* MEFs compared to *SNP309T* MEFs ($p < 0.001$) (Figure 31). To test the efficiency of transfections, we performed RT-qPCR on *FGF21* and *BRCA1* (known targets of Sp1 and E2F6, respectively) and there were no significant differences in expression between *SNP309T* MEFs compared to *SNP309G* MEFs (Figure 32). Finally, I examined protein levels of SP1 and E2F6 in thymus and keratinocytes harvested from *Mdm2*^{*SNP309G/G*} and *Mdm2*^{*SNP309T/T*} mice and showed that SP1 is expressed in thymus and not detectable in keratinocytes and vice versa, E2F6 is clearly expressed in keratinocytes but not in thymus samples (Figure 33). These differences were independent of genotype.

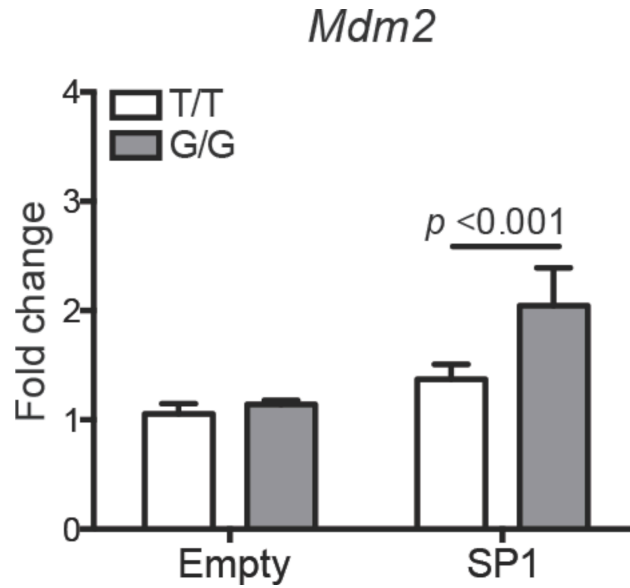


Figure 29. *Mdm2* mRNA expression in MEFs transfected with SP1. Primary MEF's from *SNP309* mice were transiently transfected with 6ug of plasmids expressing SP1 and FACS sorted with GFP. Expression levels are normalized to that of empty vector (control) samples. Statistical significance was determined by Two-way ANOVA; *Mdm2*^{*SNP309T/T*}, T/T; *Mdm2*^{*SNP309G/G*}, G/G.

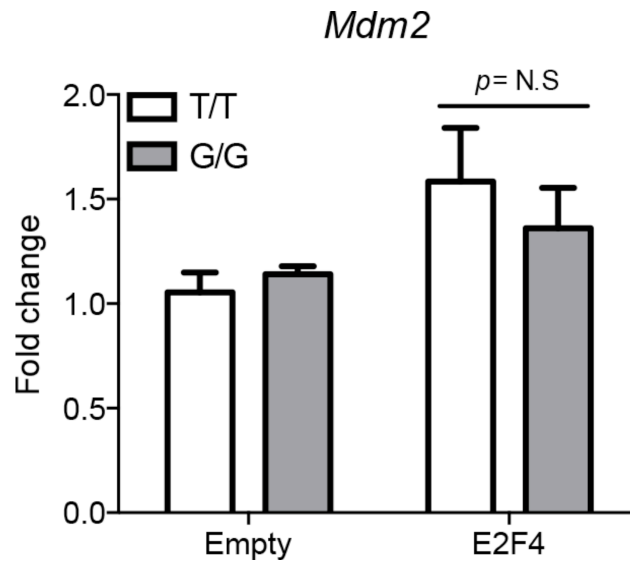


Figure 30. *Mdm2* mRNA expression in MEFs transfected with E2F4. Primary MEF's from *SNP309* mice were transiently transfected with 6μg of plasmids expressing E2F4 and FACS sorted with GFP. Expression levels are normalized to that of empty vector (control) samples. Statistical significance was determined by Two-way ANOVA; *Mdm2*^{*SNP309T/T*}, T/T; *Mdm2*^{*SNP309G/G*}, G/G; N.S= not significant.

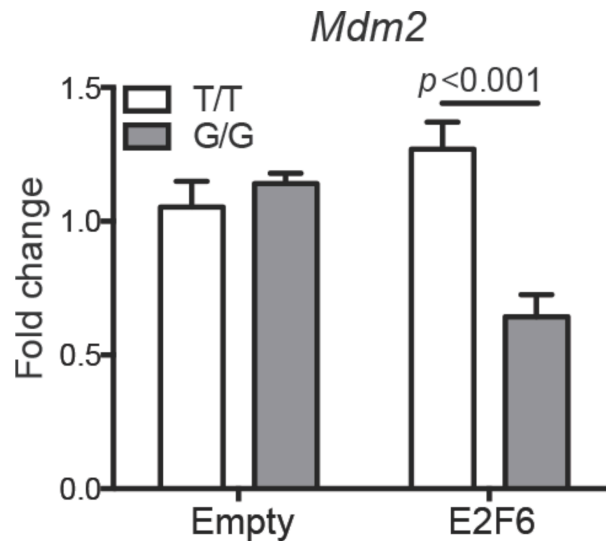


Figure 31. *Mdm2* mRNA expression in MEFs transfected with E2F6. Primary MEF's from *SNP309* mice were transiently transfected with 6ug of plasmids expressing E2F6 and FACS sorted with GFP. Expression levels are normalized to that of empty vector (control) samples. Statistical significance was determined by Two-way ANOVA; *Mdm2*^{*SNP309T/T*}, T/T; *Mdm2*^{*SNP309G/G*}, G/G.

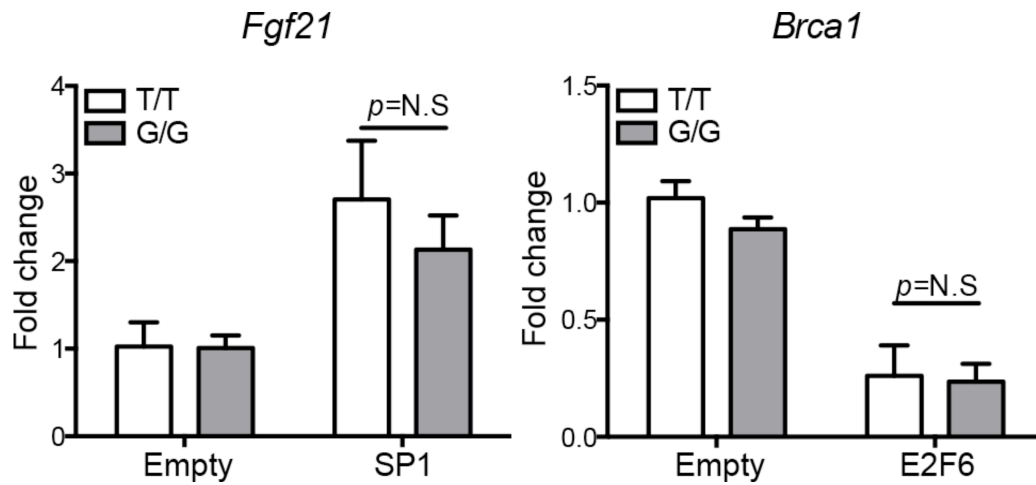


Figure 32. *Mdm2* mRNA expression in MEFs transfected with SP1 or E2F6. Primary MEF's from *SNP309* mice were transiently transfected with 6μg of plasmids expression SP1 or E2F6 and FACS sorted with GFP. Expression levels are normalized to that of empty vector (control) samples. Statistical significance was determined by Two-way ANOVA; *Mdm2*^{SNP309T/T}, T/T; *Mdm2*^{SNP309G/G}, G/G.

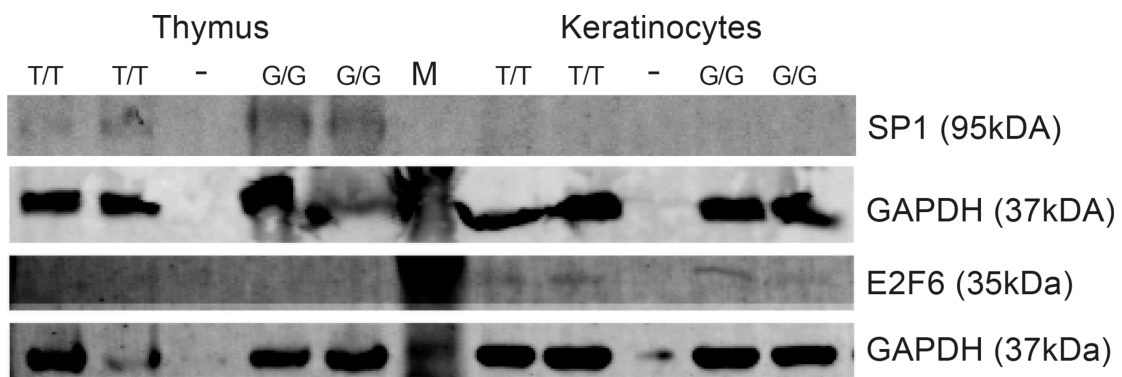


Figure 33. Protein analyses in thymi and keratinocytes of SNP309 mice. Western blot analysis of basal levels of SP1 and E2F6 proteins. Two tissues per genotype were representative of the analysis. GAPDH protein expression was used as a control. M, marker; *Mdm2*^{SNP309T/T}, T/T; *Mdm2*^{SNP309G/G}, G/G.

Transcriptional repressor E2F6 preferably binds to the *Mdm2* P2 promoter of *SNP309G* keratinocytes compared to *SNP309T* keratinocytes

We next examined the binding specificity of E2F6 to the *Mdm2*-P2 promoter in keratinocytes harvested from *SNP309* mice by performing chromatin immunoprecipitation assays (ChIP). We isolated primary keratinocytes from *Mdm2*^{*SNP309G/G*} and *Mdm2*^{*SNP309T/T*} newborn pups. ChIP with an E2F6 antibody and subsequent RT-qPCR analysis showed that E2F6 binds more significantly ($p < 0.0001$) to the *Mdm2*-P2 promoter in keratinocytes of *SNP309G* compared to *SNP309T* (Figure 34). Binding of E2F6 to the control *BRCAl* promoter (an established target of E2F6) showed no difference in *SNP309G* compared to *SNP309T*.

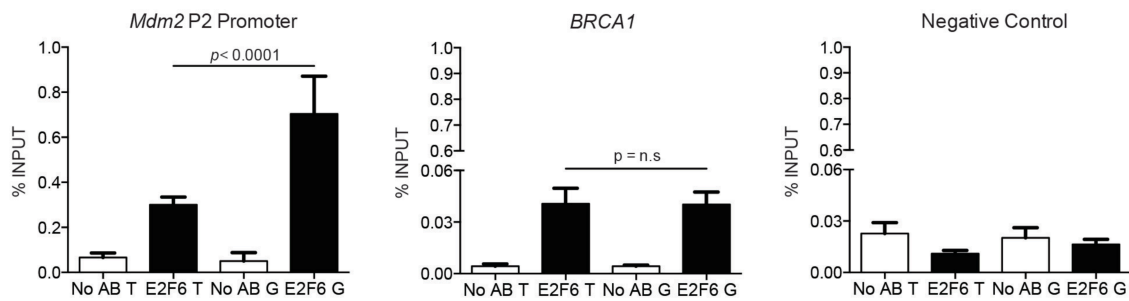


Figure 34. E2F6 ChIP analysis of the *MDM2* P2 promoter in keratinocytes of *Mdm2*^{SNP309T/T} and *Mdm2*^{SNP309G/G} mice. E2F6 ChIP assays for the *BRCA1* promoter in keratinocytes was used as positive control. A sequence downstream of the *Mdm2* promoter not thought to bind E2F6 was used as a negative control. Statistical analysis was performed using Two-way ANOVA; *Mdm2*^{SNP309T/T}, T/T; *Mdm2*^{SNP309G/G}, G/G.

Interim summary

Mdm2 basal expression in tissues from *Mdm2*^{SNP309} mice revealed contrasting differences in expression. Keratinocytes from *Mdm2*^{SNP309T/T} mice exhibit higher *Mdm2* basal expression compared to *Mdm2*^{SNP309G/G} mice in C57BL/6 and FVB strains. ChIP-seq data from ENCODE show that transcriptional repressor E2F6 binds proximal to the *MDM2* P2 promoter. Transfection experiments in cells harvested from *Mdm2*^{SNP309} mice show that E2F6 lowers *Mdm2* expression in *Mdm2*^{SNP309G/G} tissues, but does not affect *Mdm2*^{SNP309T/T} tissues. Finally, ChIP with an E2F6 antibody and subsequent RT-qPCR analysis showed that E2F6 binds more significantly to the *Mdm2*-P2 promoter in keratinocytes of *Mdm2*^{SNP309G/G} mice compared to *Mdm2*^{SNP309T/T} keratinocytes. Collectively, these data show that the *SNP309G* regulates *Mdm2* basal expression in a tissue-dependent manner utilizing alternative transcription factors.

CHAPTER III
MATERIALS AND METHODS

Chapter 3. Materials and Methods

Generation of homozygous *Mdm2*^{SNP309T/T} and *Mdm2*^{SNP309G/G} mice. (Resource previously available in the laboratory)

MD Anderson Cancer Center Institutional Animal Care and Use Committee approved all protocols on mouse experiments, and these were conducted in compliance with the guidelines of the United States Animal Welfare Act and the National Institutes of Health. The *Mdm2*^{SNP309G/G} and *Mdm2*^{SNP309T/T} mouse models were generated in our laboratory and had been previously described [119]. To generate *Mdm2*^{SNP309G/G} and *Mdm2*^{SNP309T/T} mice in FVB background strain, *Mdm2*^{SNP309G/G} and *Mdm2*^{SNP309T/T} mice in C57BL/6 background strains were backcrossed for five generations to FVB by the Johnson laboratory.

Mouse genotyping analysis

Tissues were collected from mice, either tails or ear punch, and were first genotyped for *Mdm2* alleles using a previously described protocol [66, 149]. The forward primer (5'- GCATTAGAGAGTGGTCACTGCGAC-3') reverse primer (5'- GAACAGTGATAGAACATCATGTCAC-3') were used. PCR conditions: 95°C for 5 minutes for preheating, followed by 95°C 1 minute, 54°C 45 seconds, 72°C 1 minute, (steps 2-4 were repeated for 40 cycles), and 72C for 8 minutes for elongation. Bands were identified at 150 base pairs. After genotyping, DNA from *Mdm2*^{SNP309G/G} and *Mdm2*^{SNP309T/T} mice were randomly sequenced using Sanger-based DNA sequencing to confirm the presence of the G or T nucleotide using primers within the *MDM2* P2 promoter using forward (5'-GGATTTCGGACGGCTCTCG-3') and reverse (5'-

CGCGCAGCGTTCACACTAG-3') primers. The sequencing was performed by the Sequencing and Microarray Facility (SMF) at the University of Texas M.D. Anderson Cancer Center using the forward and reserve primers.

Environmental stress treatments

In the ionizing radiation study, we generated cohorts of *Mdm2*^{SNP309G/G} and *Mdm2*^{SNP309T/T} mice in the C57BL/6 strain background and treated the cohorts with 1Gy ionizing radiation two days after birth as a model for environmental stress. Cohorts of non-treated *Mdm2*^{SNP309G/G} and *Mdm2*^{SNP309T/T} mice were also generated as controls. I monitored daily spontaneous tumor susceptibility in treated and non-treated cohorts and mice were sacrificed upon tumor formation.

For the skin carcinogenesis study, we generated cohorts of *Mdm2*^{SNP309G/G} and *Mdm2*^{SNP309T/T} mice in the skin tumor prone FVB background strain and treated the cohort with a skin carcinogenesis regimen, including UVB and B(a)P, as previously described [144, 150]. Non-treated *Mdm2*^{SNP309G/G} and *Mdm2*^{SNP309T/T} mice were used as controls.

UVB regimen

The dorsal skins of young adult (six to eight week old) *Mdm2*^{SNP309G/G} and *Mdm2*^{SNP309T/T} mice were shaved and one day later exposed to gradually increasing doses of UVB radiation (100- 341 mJ/cm²) three times per week for 30 weeks. Mice were monitored and tumors recorded for an additional ten weeks before all mice were sacrificed.

B(a)P regimen

The dorsal skins of young adult *Mdm2*^{SNP309G/G} and *Mdm2*^{SNP309T/T} mice were shaved and one day later B(a)P dissolved in acetone (317 nmol) was applied to the shaved area. This treatment continued once a week for 30 weeks. Mice were monitored for an additional ten weeks before all mice were sacrificed.

Histopathology and Immunohistochemistry

Histological preparation and immunohistochemistry (IHC) were conducted as a collaborative effort between Dr. Lozano and Dr. Johnson's laboratories.

Dr. Lozano's laboratory

Mouse tissues were harvested from euthanized mice and washed in cold phosphate buffered saline (PBS) and fixed in 10% formalin for 48 hours. Histological processing and hematoxylin and eosin (H&E) were performed by the Department of Veterinary Medicine at the University of Texas M.D. Anderson Cancer Center. Tissues were sectioned into slices with 6 μ M thickness. Immunohistochemistry was performed on paraffin-embedded tissues as previously described [151], using antibodies for cleaved caspase-3 (1:200, Cell Signalling Technology, Asp 175), CD3 (1:100, Abcam, ab5690), B220 (1:100, BD Pharmigen, 530286) and p21-WAF1-Cip1 (1:200, Dako, M7202). Stain sections were detected with Vectastain Elite ABC Reagent and Vector DAB substrate (Vector Laboratories, PK-6100)

Dr. Johnson's laboratory

Tissue processing and immunohistochemistry were performed by the MD Anderson Cancer Center, Science Park Histology Core. Briefly, dorsal skin samples were fixed in

10% formalin for 24 h, paraffin-embedded, sectioned and stained for p53 (Novocastra #NCL-p53-CM5p). Digital images of stained sections were captured using the Aperio ScanScope CS slide scanner and the numbers of positive cells in the epidermis were counted using the manufacturer's GENIE software (Aperio Technologies, Vista, CA).

Western Blot analysis

Protein lysates were prepared by lysing thymi or keratinocytes from *SNP309* mice in NP-40 buffer. Protein estimation was carried out with BCA (Pierce #23225). One hundred micrograms of lysate were resolved on 10% SDS-PAGE and transferred to nitrocellulose membranes and immunoblotted with antibodies against SP1 (1:200; Santa Cruz, #sc-59), E2F6 (1:200; Santa Cruz #E-20), and GAPDH (1:1000; Abcam #ab9485). Western blots were repeated at least three times with biological replicates. The membranes were incubated with IRDye@800 conjugated goat anti-rabbit IgG (1:10,000; LI-COR, #926-3211) or IRDye@680LT conjugated donkey anti-mouse IgG (1:10,000; LI-COR, #926-68022) the membranes were scanned with ODYSSEY CLx Infrared Imaging System.

Real-Time RT-PCR

Fresh tissues were necropsied from mice and flash frozen. Total RNA was isolated using TRIZOL reagent (Invitrogen, 15596-026) following the manufacturer's instructions. The RNA was treated with DNase I (Roche, 0416728-001) and reverse

transcribed using the product protocol (GE Healthcare, 27-9261). Real-Time RT-PCR using SYBR green (BioRad, 1725270) was performed on a 7900HT Fast Real-time PCR system (Applied Biosystems) using a method previously described [152]. Expression was normalized to Rplp0.

Primary cell cultures

Keratinocytes

Primary keratinocytes were isolated from the epidermis of two-day-old *Mdm2*^{SNP309G/G} and *Mdm2*^{SNP309T/T} pups. The pups were decapitated and washed with PBS and rinsed in 70% ethanol. The pups were skinned, and the skin layer was digested with dispase (1500 unit/ml, Becton Dickinson, 354235) overnight at 4°C. After digestion, the epidermis was isolated, minced and vigorously shaken in DMEM containing 10% FBS before it was passed through a 70 µm mesh filter. To improve yields and control for sample variability, we pooled epidermis from multiple mice harboring the same genotype. We plated 1X10⁷ cells in 10 cm dishes in Waymouth's MB752/1 media (Life Technologies, 11220-035) for 3h, and then replaced the media with KGM-2 media (Lonza, CC-3108). Keratinocytes were ready for experiments after three days.

Mouse embryonic fibroblasts (MEFs)

MEFs were harvested from 13.5-day embryos of *Mdm2*^{SNP309G/G} and *Mdm2*^{SNP309T/T} genotype as previously described [76]. MEFs were cultured in Dulbecco's modified Eagle's medium (Thermo Fisher, 11965-092) supplemented with 10% FBS and penicillin-streptomycin (100 IU/ml, 100 ugs/ml respectively). Only low-passage MEFs

were used for experiments (< P4). Early passage MEFs were transfected with seven µg of pCMV-GFP vector containing E2F6 cDNA, SP1 cDNA, or empty vector using Lipofectamine 3000 reagent (Sigma, L3000015). Forty-eight hours later, GFP-positive cells were sorted by FACS and RNA was extracted for RT-PCR analysis.

Chromatin immunoprecipitation assay

The Chromatin immunoprecipitation assay was executed as previously described [153]. The E2F6 Antibody (Santa Cruz Biotechnology, E-20) was previously characterized for chromatin immunoprecipitation [154]. The chromatin was cross-linked with 37% formaldehyde for 10 minutes, and the fixation was terminated by the addition of 2M glycine. The cells were harvested in SDS buffer (100 mM NaCl; 50 mM Tris-HCl, pH 8.1; 5 mM EDTA, pH 8.0; 0.02% NaN₃; and 0.5% SDS, plus protease inhibitors) and pelleted. The pellets were resuspended in 0.75 ml (per T150 flask) ice-cold immunoprecipitation (IP) buffer (100 mM Tris, pH 8.6; 0.3% SDS; 1.7% Triton X-100; 5 mM EDTA) and sonicated by pulsing 5 times for 20 s at power setting 3 and 100% duty cycle on a Branson Sonifier 450. Sonication average length of 300 to 1,000 bp was confirmed by agarose gel electrophoresis. The Bradford protein assay was performed as previously described [153] to quantify the immunoprecipitation concentration and aliquots of 1.5mg of protein were prepared in IP buffer. The aliquots were pre-cleared with 25µl of salmon sperm/protein A agarose beads (Millipore SIGMA, 16-157C). 25ul of each aliquot was saved as an input control. The primary antibody (2 µg) was added overnight at 4°C. Salmon sperm/protein A agarose was added to the immune complexes.

The input controls and washed immune complex pellets were resuspended in 250µl of 1% SDS, 0.1 M NaHCO₃, and the samples were incubated overnight at 65°C to elute the immune complexes and to reverse the cross-links. The digestion with proteinase K was performed as previously described [153] and the samples were resuspended in 300µl of H₂O. Real-time PCR was performed as previously described [152]. Primers were designed using primer express software (<http://home.appliedbiosystems.com>). Data was presented as percentages of the total, calculated exactly as previously published [152].

Statistical analysis

All comparisons were analyzed using GraphPad Prism version 6.00 (GraphPad Software, La Jolla California USA). Gene expression analysis comparing untreated to treated samples was determined by two-way analysis of variance (ANOVA), and the comparison of basal expression between the two genotypes was determined by student's t-test. Tumor-free survival was determined using Log-Rank test and differences in tumor spectrum and tumor multiplicity with Fisher's exact test. A *p*-value of <0.05 was considered statistically significant.

CHAPTER IV
DISCUSSION & FUTURE DIRECTIONS

Chapter 4. Discussion and Future Directions

Discussion

Functional polymorphisms alter gene function and can lead to disease risk. Environmental factors can have synergistic effects on disease-associated SNPs and exacerbate the outcome; however cooperative mechanisms between functional polymorphisms and environmental factors have not been well defined. In my thesis work, I utilized a well-known functional polymorphism involved in the p53 pathway, *SNP309*, to investigate gene-environment interactions in modulating tumor susceptibility. Previous data investigated the influence of the *SNP309G* on tumor risk. Mouse models harboring the *Mdm2*^{*SNP309*} alleles were genetically engineered and examined for tumor susceptibility. The data show that *Mdm2*^{*SNP309G/G*} mice are more susceptible to spontaneous tumor formation and exhibit a significantly lower overall survival compared to *Mdm2*^{*SNP309T/T*} mice [119]. Furthermore, tissues from *Mdm2*^{*SNP309G/G*} mice show significantly higher *Mdm2* expression and exhibit decrease apoptotic response compared to *Mdm2*^{*SNP309T/T*} tissues. Consequently, the p53 pathway is attenuated in tissues from *Mdm2*^{*SNP309G/G*} mice. Thus, these data determined that the *SNP309G* allele has a direct impact on tumor risk [119]. To study the effects of environmental factors and the *SNP309G* allele in tumor risk, I challenged *Mdm2*^{*SNP309T/T*} and *Mdm2*^{*SNP309G/G*} mice with established environmental stresses that promote cancer risk and affect the p53 pathway. Furthermore, these models are relevant to human health: people are consistently exposed to low dose IR via cosmic rays and medical imaging procedures [133], UV from the sun [139], and the B(a)P carcinogen from smoking [155].

My results show that *SNP309G* allele exacerbated tumor risk in *Mdm2*^{*SNP309G/G*} mice compared to *Mdm2*^{*SNP309T/T*} mice after low-dose IR treatment. These results support previous data [119], which show that the *Mdm2*^{*SNP309G/G*} mice have increased susceptibility to tumors compared to *Mdm2*^{*SNP309T/T*} mice, affirming that *SNP309G* is an ‘at risk’ allele for spontaneous tumor formation. In contrast, *Mdm2*^{*SNP309T/T*} mice exhibit increased risk of skin squamous cell carcinoma compared to *Mdm2*^{*SNP309G/G*} mice after UVB or B(a)P treatment. Overall, these results suggest that environmental factors and cellular factors cooperate to promote cancer risk in a tissue-dependent manner.

***Mdm2* expression differences in tumor-prone tissues**

The differences in tumor risk between *Mdm2*^{*SNP309T/T*} and *Mdm2*^{*SNP309G/G*} mice suggested tissue-specific differences in their regulation of the p53 pathway. To further understand these conflicting results, I first evaluated p53 activity in response to insult in tumor-prone tissues. In the low-dose IR study, spleen and thymus from *Mdm2*^{*SNP309G/G*} mice show increased *Mdm2* expression and dampened p53 activity post-IR treatment compared to irradiated tissues from *Mdm2*^{*SNP309T/T*} mice and to non-irradiated mice. Furthermore, the data showed that *Mdm2*^{*SNP309G/G*} mouse lymphatic tissues exhibit a delay in activation of apoptosis compared to *Mdm2*^{*SNP309T/T*} after low-dose IR. Previous data show that Akt signaling pathway delays p53-mediated apoptosis [156], suggesting crosstalk between p53, Mdm2, and Akt pathways affect program cell death [157].

In contrast, both UVB and B(a)P skin carcinogenesis models in an FVB background demonstrated the opposite effect and highlighted increased *Mdm2* expression and attenuated p53 activity in the epidermal skin cells of *Mdm2*^{SNP309T/T} mice compared to *Mdm2*^{SNP309G/G} mice. These contrasting results can be explained by the opposing differences in *Mdm2* basal expression in lymphatic and epidermal skin tissues, thus resulting in tissue-specific differences in steady state levels of p53 and transactivation of p53 targets in response to insult.

The IR and UVB/B(a)P experiments were performed in C57BL/6 and FVB background strains, respectively, exposing the possibility that observed differences were strain-specific. Thus, I investigated the effects of mouse strain on *Mdm2* expression of keratinocytes from *Mdm2*^{SNP309} mice in C57BL/6 and FVB background strains. The data showed that keratinocytes from *Mdm2*^{SNP309T/T} mice exhibit higher *Mdm2* basal expression levels compared to *Mdm2*^{SNP309G/G} mice independent of mouse strain. Moreover, fibroblasts from *Mdm2*^{SNP309G/G} FVB mice showed relatively higher *Mdm2* basal expression levels compared to fibroblasts from *Mdm2*^{SNP309T/T} FBV mice. These data are consistent with previous experiments conducted in C57BL/6 mice. Thus, mouse strain did not affect *SNP309*-dependent *Mdm2* regulation in epidermal skin tissue and fibroblasts.

Another factor that we investigated was the effect of DNA damage on *Mdm2* expression on different cell-types from *Mdm2*^{SNP309} mice. Exposure to UVB further increased *Mdm2* expression levels of keratinocytes from *Mdm2*^{SNP309T/T} mice compared to *Mdm2*^{SNP309G/G} keratinocytes. Thus, we examined the effects of UVB on fibroblast cells

from *Mdm2*^{SNP309} FVB mice. The data show fibroblasts from *Mdm2*^{SNP309G/G} FVB mice exhibit significantly higher *Mdm2* expression levels compared to fibroblasts from *Mdm2*^{SNP309T/T} mice after UVB treatment. Thus, these data indicate that the *Mdm2* expression levels differences are not insult dependent.

A further examination of basal *Mdm2* expression from different tissues harvested from *SNP309* mice in a C57BL/6 background revealed considerable variation in *Mdm2* expression levels between tissues and within genotypes of *SNP309* mice. Furthermore, there are some differences in *Mdm2* expression between genders, suggesting that other factors cooperate with the *SNP309* allele and alter *Mdm2* expression in a tissue-dependent manner through discrete mechanisms.

The differences in *Mdm2* expression between tissues were a surprise. *Mdm2* expression levels have not been thoroughly examined in all tissues, especially in normal samples. However, there is evidence from other ubiquitously expressed genes suggesting expression differences in different tissues. Previous studies, which have focused on characterizing and understanding the gene and protein spatial distributions in normal and diseased tissues, corroborate these finding: gene expression signatures vary among tissues [158, 159]. These results have been studied in healthy and diseased tissues of human and mice. Furthermore, the expression atlas (<http://www.ebi.ac.uk/gxa/home>) and protein atlas (<http://www.proteinatlas.org>) [160, 161] reveal gene and protein expression variation between tissues of human and mice. However, to my knowledge, no studies have demonstrated that a functional SNP contrastingly alters gene expression in tissues of the same organism. Thus, this is a novel observation.

The *SNP309G* allele cooperates with epidermal cell factors to regulate *Mdm2* expression in skin tissue

To understand the mechanism(s) that regulates *SNP309*-dependent *Mdm2* expression in epidermal skin tissue, I evaluated the transcription factors that regulate *Mdm2* expression through the *Mdm2* P2 promoter in keratinocytes from *SNP309* mice. The ChIP-seq data from ENCODE confirmed that E2F6 binds to the *MDM2*-P2 promoter in cells expressing *SNP309T/G* alleles, harboring its binding signature adjacent to the *SNP309* site, suggesting that E2F6 may have a role in *SNP309*-dependent *Mdm2* expression regulation.

Our data show that *Mdm2* expression in keratinocytes is controlled by the *SNP309G* allele through an E2F6 suppressive mechanism. Previous mechanistic studies both in human and mouse tissues show that SP1 preferentially binds to *SNP309G* allele to increase *Mdm2* expression [107, 119]. Thus, I examined the role of SP1 on *Mdm2* expression regulation. Overexpression of SP1 in MEFs harvested from *Mdm2*^{*SNP309T/T*} and *Mdm2*^{*SNP309G/G*} mice show upregulation of *Mdm2* expression in MEFs from *Mdm2*^{*SNP309G/G*} mice, but there was no increase in *Mdm2* expression in *Mdm2*^{*SNP309T/T*} MEFs. In contrast, E2F6 overexpression experiments show preferential suppression of *Mdm2* levels in MEFs harboring the *SNP309G* allele. Moreover, our ChIP assay confirmed that E2F6 preferentially binds to the *Mdm2*-P2 promoter in keratinocytes of *SNP309G* compared to *SNP309T*, suggesting that the *SNP309G* allele contrastingly alters *Mdm2* expression depending on the transcription factor-*Mdm2* P2 interactions. Furthermore, these contrasting differences in *Mdm2* gene expression will dictate p53

function and stability. Thus, the *SNP309G* allele can exhibit tumor promoting, or tumor protective signatures in tissues depending on the *SNP309G*-dependent mechanism elicited to regulate *Mdm2* expression.

Our study shows that *SNP309* directly alters basal *Mdm2* expression in a cell-type dependent manner. Gene expression varies between tissues [162, 163]. Functional SNPs affect gene expression. However, most studies focus on how these variants alter gene function in the context of disease. This study is novel because we explore how functional SNPs alter gene function in normal tissues within the same organism; furthermore, we investigate discrete mechanisms that contrastingly regulate *Mdm2* expression in an *SNP309*-dependent manner. To our knowledge, this is the first time a study reports how a functional SNP utilizes separate mechanisms to alter gene regulation in the same healthy organism.

Clinical implications

To date, epidemiological studies do not associate *MDM2 SNP309* with skin squamous cell carcinoma risk [164]; thus, it is possible that our results are particular to skin keratinocytes from mice. However, many meta-analyses associating *MDM2 SNP309* to cancer risk are conflicting, even in larger studies, suggesting that other factors can promote tumor risk. We also observed differences in expression when we stratified by gender, thus, supporting the hypothesis that other factors cooperate to alter gene expression in an SNP-dependent manner in different tissues. Our study expands our understanding of how *SNP309* modulates *Mdm2* function in healthy tissues. Thus, we

examined the tumor risk in skin tissues to validate the expression differences and define a discrete mechanism in *SNP309* gene function. Furthermore, it is possible that the cohorts used in human studies harbor other SNPs within the *MDM2* promoter that give a protective advantage to *MDM2 SNP309*, as in the case of *MDM2 SNP285*, a SNP that negates the effects of *SNP309G* and protects against tumor risk [117].

Future directions

Characterizing factors that affect SNP-dependent mechanism

Functional polymorphisms are located within regulatory or protein coding sequences and alter gene regulation and influence disease risk [89-94]. Meta-analyses associate many SNPs with disease risk, but in most cases detailed molecular mechanisms have not been elucidated. Thus, the role of functional polymorphisms as clinical prognostic markers has not been fully appreciated.

There is evidence suggesting that cooperating factors influence SNP-dependent gene regulation. Many meta-analyses associating SNPs and disease are stratified by factors, such as race, gender, and age; yet, these data are sometimes contradicting when comparing to other study cohorts. Thus, it is important to understand the influence of cooperating factors by studying their molecular mechanisms in robust, controlled, and otherwise isogenic experimental systems.

In this study, we examined the role of environmental stress on *Mdm2*^{SNP309} mice. Our data show that environmental stress cooperates with the *SNP309* to promote cancer risk. More importantly, our study suggests that *Mdm2* *SNP309* regulates *Mdm2* expression in a tissue-dependent manner. To our knowledge, this is the first study that shows contrasting differences in *Mdm2* basal expression within the same organism, thus, highlighting the novelty of our findings. Furthermore, our data demonstrate that gender cooperates with *SNP309*-dependent *Mdm2* regulation. This was evident when we examined other tissues besides skin and lymphatic tissues. Thus, further mechanistic

studies evaluating the regulatory influence of gender could yield important information that could be beneficial to clinical applications.

Summary

Meta-analysis studies associating functional polymorphisms and disease risk are important tools to evaluate study cohorts. However other factors, such as environmental stress, race, and gender may influence the effects of these SNPs within a study cohort. Furthermore, SNPs may influence tissue-specific gene regulation. Thus, further characterization of SNP-dependent regulation is needed to effectively evaluate the significance of functional polymorphisms on disease risk.

Bibliography

1. Lane, D. P. 1992. Cancer. p53, guardian of the genome. *Nature* 358: 15-16.
2. Lane, D. P., and L. V. Crawford. 1979. T antigen is bound to a host protein in SV40-transformed cells. *Nature* 278: 261-263.
3. Linzer, D. I., and A. J. Levine. 1979. Characterization of a 54K dalton cellular SV40 tumor antigen present in SV40-transformed cells and uninfected embryonal carcinoma cells. *Cell* 17: 43-52.
4. Chang, C., D. T. Simmons, M. A. Martin, and P. T. Mora. 1979. Identification and partial characterization of new antigens from simian virus 40-transformed mouse cells. *Journal of virology* 31: 463-471.
5. Mercer, W. E., C. Avignolo, and R. Baserga. 1984. Role of the p53 protein in cell proliferation as studied by microinjection of monoclonal antibodies. *Molecular and cellular biology* 4: 276-281.
6. Mercer, W. E., D. Nelson, A. B. DeLeo, L. J. Old, and R. Baserga. 1982. Microinjection of monoclonal antibody to protein p53 inhibits serum-induced DNA synthesis in 3T3 cells. *Proceedings of the National Academy of Sciences of the United States of America* 79: 6309-6312.
7. Reich, N. C., and A. J. Levine. 1984. Growth regulation of a cellular tumour antigen, p53, in nontransformed cells. *Nature* 308: 199-201.

8. Jenkins, J. R., K. Rudge, and G. A. Currie. 1984. Cellular immortalization by a cDNA clone encoding the transformation-associated phosphoprotein p53. *Nature* 312: 651-654.
9. Eliyahu, D., A. Raz, P. Gruss, D. Givol, and M. Oren. 1984. Participation of p53 cellular tumour antigen in transformation of normal embryonic cells. *Nature* 312: 646-649.
10. Parada, L. F., H. Land, R. A. Weinberg, D. Wolf, and V. Rotter. 1984. Cooperation between gene encoding p53 tumour antigen and ras in cellular transformation. *Nature* 312: 649-651.
11. Jenkins, J. R., K. Rudge, P. Chumakov, and G. A. Currie. 1985. The cellular oncogene p53 can be activated by mutagenesis. *Nature* 317: 816-818.
12. Finlay, C. A., P. W. Hinds, and A. J. Levine. 1989. The p53 proto-oncogene can act as a suppressor of transformation. *Cell* 57: 1083-1093.
13. Eliyahu, D., D. Michalovitz, S. Eliyahu, O. Pinhasi-Kimhi, and M. Oren. 1989. Wild-type p53 can inhibit oncogene-mediated focus formation. *Proceedings of the National Academy of Sciences of the United States of America* 86: 8763-8767.
14. Baker, S. J., E. R. Fearon, J. M. Nigro, S. R. Hamilton, A. C. Preisinger, J. M. Jessup, P. vanTuinen, D. H. Ledbetter, D. F. Barker, Y. Nakamura, R. White, and B. Vogelstein. 1989. Chromosome 17 deletions and p53 gene mutations in colorectal carcinomas. *Science* 244: 217-221.

15. Donehower, L. A., M. Harvey, B. L. Slagle, M. J. McArthur, C. A. Montgomery, Jr., J. S. Butel, and A. Bradley. 1992. Mice deficient for p53 are developmentally normal but susceptible to spontaneous tumours. *Nature* 356: 215-221.
16. Zilfou, J. T., and S. W. Lowe. 2009. Tumor suppressive functions of p53. *Cold Spring Harbor perspectives in biology* 1: a001883.
17. el-Deiry, W. S., T. Tokino, V. E. Velculescu, D. B. Levy, R. Parsons, J. M. Trent, D. Lin, W. E. Mercer, K. W. Kinzler, and B. Vogelstein. 1993. WAF1, a potential mediator of p53 tumor suppression. *Cell* 75: 817-825.
18. el-Deiry, W. S., S. E. Kern, J. A. Pietenpol, K. W. Kinzler, and B. Vogelstein. 1992. Definition of a consensus binding site for p53. *Nature genetics* 1: 45-49.
19. Bargonetti, J., P. N. Friedman, S. E. Kern, B. Vogelstein, and C. Prives. 1991. Wild-type but not mutant p53 immunopurified proteins bind to sequences adjacent to the SV40 origin of replication. *Cell* 65: 1083-1091.
20. Kern, S. E., K. W. Kinzler, A. Bruskin, D. Jarosz, P. Friedman, C. Prives, and B. Vogelstein. 1991. Identification of p53 as a sequence-specific DNA-binding protein. *Science* 252: 1708-1711.
21. Pavletich, N. P., K. A. Chambers, and C. O. Pabo. 1993. The DNA-binding domain of p53 contains the four conserved regions and the major mutation hot spots. *Genes & development* 7: 2556-2564.
22. Friedman, P. N., X. Chen, J. Bargonetti, and C. Prives. 1993. The p53 protein is an unusually shaped tetramer that binds directly to DNA. *Proceedings of the National Academy of Sciences of the United States of America* 90: 3319-3323.

23. Wang, P., M. Reed, Y. Wang, G. Mayr, J. E. Stenger, M. E. Anderson, J. F. Schwedes, and P. Tegtmeier. 1994. p53 domains: structure, oligomerization, and transformation. *Molecular and cellular biology* 14: 5182-5191.
24. Vogelstein, B., D. Lane, and A. J. Levine. 2000. Surfing the p53 network. *Nature* 408: 307-310.
25. Vousden, K. H., and X. Lu. 2002. Live or let die: the cell's response to p53. *Nature reviews. Cancer* 2: 594-604.
26. Motoyama, N., and K. Naka. 2004. DNA damage tumor suppressor genes and genomic instability. *Current opinion in genetics & development* 14: 11-16.
27. Lowe, S. W., E. M. Schmitt, S. W. Smith, B. A. Osborne, and T. Jacks. 1993. p53 is required for radiation-induced apoptosis in mouse thymocytes. *Nature* 362: 847-849.
28. Kastan, M. B., Q. Zhan, W. S. el-Deiry, F. Carrier, T. Jacks, W. V. Walsh, B. S. Plunkett, B. Vogelstein, and A. J. Fornace, Jr. 1992. A mammalian cell cycle checkpoint pathway utilizing p53 and GADD45 is defective in ataxia-telangiectasia. *Cell* 71: 587-597.
29. Raycroft, L., H. Y. Wu, and G. Lozano. 1990. Transcriptional activation by wild-type but not transforming mutants of the p53 anti-oncogene. *Science* 249: 1049-1051.
30. Miyashita, T., and J. C. Reed. 1995. Tumor suppressor p53 is a direct transcriptional activator of the human bax gene. *Cell* 80: 293-299.

31. Brady, C. A., and L. D. Attardi. 2010. p53 at a glance. *Journal of cell science* 123: 2527-2532.
32. Jiang, L., N. Kon, T. Li, S. J. Wang, T. Su, H. Hibshoosh, R. Baer, and W. Gu. 2015. Ferroptosis as a p53-mediated activity during tumour suppression. *Nature* 520: 57-62.
33. Crichton, D., S. Wilkinson, J. O'Prey, N. Syed, P. Smith, P. R. Harrison, M. Gasco, O. Garrone, T. Crook, and K. M. Ryan. 2006. DRAM, a p53-induced modulator of autophagy, is critical for apoptosis. *Cell* 126: 121-134.
34. Vousden, K. H., and K. M. Ryan. 2009. p53 and metabolism. *Nature reviews. Cancer* 9: 691-700.
35. Vousden, K. H., and C. Prives. 2009. Blinded by the Light: The Growing Complexity of p53. *Cell* 137: 413-431.
36. Levine, A. J., and M. Oren. 2009. The first 30 years of p53: growing ever more complex. *Nature reviews. Cancer* 9: 749-758.
37. Allton, K., A. K. Jain, H. M. Herz, W. W. Tsai, S. Y. Jung, J. Qin, A. Bergmann, R. L. Johnson, and M. C. Barton. 2009. Trim24 targets endogenous p53 for degradation. *Proceedings of the National Academy of Sciences of the United States of America* 106: 11612-11616.
38. Wang, X., M. Zha, X. Zhao, P. Jiang, W. Du, A. Y. Tam, Y. Mei, and M. Wu. 2013. Siva1 inhibits p53 function by acting as an ARF E3 ubiquitin ligase. *Nature communications* 4: 1551.

39. Dornan, D., I. Wertz, H. Shimizu, D. Arnott, G. D. Frantz, P. Dowd, K. O'Rourke, H. Koeppen, and V. M. Dixit. 2004. The ubiquitin ligase COP1 is a critical negative regulator of p53. *Nature* 429: 86-92.
40. Hakem, A., M. Bohgaki, B. Lemmers, E. Tai, L. Salmena, E. Matysiak-Zablocki, Y. S. Jung, J. Karaskova, L. Kaustov, S. Duan, J. Madore, P. Boutros, Y. Sheng, M. Chesi, P. L. Bergsagel, B. Perez-Ordóñez, A. M. Mes-Masson, L. Penn, J. Squire, X. Chen, I. Jurisica, C. Arrowsmith, O. Sanchez, S. Benchimol, and R. Hakem. 2011. Role of Pirh2 in mediating the regulation of p53 and c-Myc. *PLoS genetics* 7: e1002360.
41. Karni-Schmidt, O., M. Lokshin, and C. Prives. 2016. The Roles of MDM2 and MDMX in Cancer. *Annual review of pathology* 11: 617-644.
42. Cahilly-Snyder, L., T. Yang-Feng, U. Francke, and D. L. George. 1987. Molecular analysis and chromosomal mapping of amplified genes isolated from a transformed mouse 3T3 cell line. *Somatic cell and molecular genetics* 13: 235-244.
43. Jones, S. N., A. E. Roe, L. A. Donehower, and A. Bradley. 1995. Rescue of embryonic lethality in Mdm2-deficient mice by absence of p53. *Nature* 378: 206-208.
44. Montes de Oca Luna, R., D. S. Wagner, and G. Lozano. 1995. Rescue of early embryonic lethality in mdm2-deficient mice by deletion of p53. *Nature* 378: 203-206.

45. Grier, J. D., S. Xiong, A. C. Elizondo-Fraire, J. M. Parant, and G. Lozano. 2006. Tissue-specific differences of p53 inhibition by Mdm2 and Mdm4. *Molecular and cellular biology* 26: 192-198.
46. Xiong, S., C. S. Van Pelt, A. C. Elizondo-Fraire, G. Liu, and G. Lozano. 2006. Synergistic roles of Mdm2 and Mdm4 for p53 inhibition in central nervous system development. *Proceedings of the National Academy of Sciences of the United States of America* 103: 3226-3231.
47. Momand, J., G. P. Zambetti, D. C. Olson, D. George, and A. J. Levine. 1992. The mdm-2 oncogene product forms a complex with the p53 protein and inhibits p53-mediated transactivation. *Cell* 69: 1237-1245.
48. Oliner, J. D., K. W. Kinzler, P. S. Meltzer, D. L. George, and B. Vogelstein. 1992. Amplification of a gene encoding a p53-associated protein in human sarcomas. *Nature* 358: 80-83.
49. Haupt, Y., R. Maya, A. Kazaz, and M. Oren. 1997. Mdm2 promotes the rapid degradation of p53. *Nature* 387: 296-299.
50. Kubbutat, M. H., S. N. Jones, and K. H. Vousden. 1997. Regulation of p53 stability by Mdm2. *Nature* 387: 299-303.
51. Honda, R., H. Tanaka, and H. Yasuda. 1997. Oncoprotein MDM2 is a ubiquitin ligase E3 for tumor suppressor p53. *FEBS letters* 420: 25-27.
52. Barak, Y., E. Gottlieb, T. Juven-Gershon, and M. Oren. 1994. Regulation of mdm2 expression by p53: alternative promoters produce transcripts with nonidentical translation potential. *Genes & development* 8: 1739-1749.

53. Juven, T., Y. Barak, A. Zauberman, D. L. George, and M. Oren. 1993. Wild type p53 can mediate sequence-specific transactivation of an internal promoter within the mdm2 gene. *Oncogene* 8: 3411-3416.
54. Landers, J. E., S. L. Cassel, and D. L. George. 1997. Translational enhancement of mdm2 oncogene expression in human tumor cells containing a stabilized wild-type p53 protein. *Cancer research* 57: 3562-3568.
55. Perry, M. E., J. Piette, J. A. Zawadzki, D. Harvey, and A. J. Levine. 1993. The mdm-2 gene is induced in response to UV light in a p53-dependent manner. *Proceedings of the National Academy of Sciences of the United States of America* 90: 11623-11627.
56. Barak, Y., T. Juven, R. Haffner, and M. Oren. 1993. mdm2 expression is induced by wild type p53 activity. *The EMBO journal* 12: 461-468.
57. Pant, V., S. Xiong, J. G. Jackson, S. M. Post, H. A. Abbas, A. Quintas-Cardama, A. N. Hamir, and G. Lozano. 2013. The p53-Mdm2 feedback loop protects against DNA damage by inhibiting p53 activity but is dispensable for p53 stability, development, and longevity. *Genes & development* 27: 1857-1867.
58. Marine, J. C., and A. G. Jochemsen. 2005. Mdmx as an essential regulator of p53 activity. *Biochemical and biophysical research communications* 331: 750-760.
59. Sharp, D. A., S. A. Kratowicz, M. J. Sank, and D. L. George. 1999. Stabilization of the MDM2 oncoprotein by interaction with the structurally related MDMX protein. *The Journal of biological chemistry* 274: 38189-38196.

60. Parant, J., A. Chavez-Reyes, N. A. Little, W. Yan, V. Reinke, A. G. Jochemsen, and G. Lozano. 2001. Rescue of embryonic lethality in Mdm4-null mice by loss of Trp53 suggests a nonoverlapping pathway with MDM2 to regulate p53. *Nature genetics* 29: 92-95.
61. Migliorini, D., E. Lazzerini Denchi, D. Danovi, A. Jochemsen, M. Capillo, A. Gobbi, K. Helin, P. G. Pelicci, and J. C. Marine. 2002. Mdm4 (Mdmx) regulates p53-induced growth arrest and neuronal cell death during early embryonic mouse development. *Molecular and cellular biology* 22: 5527-5538.
62. Finch, R. A., D. B. Donoviel, D. Potter, M. Shi, A. Fan, D. D. Freed, C. Y. Wang, B. P. Zambrowicz, R. Ramirez-Solis, A. T. Sands, and N. Zhang. 2002. mdmx is a negative regulator of p53 activity in vivo. *Cancer research* 62: 3221-3225.
63. Soussi, T., and G. Lozano. 2005. p53 mutation heterogeneity in cancer. *Biochemical and biophysical research communications* 331: 834-842.
64. Cheok, C. F., C. S. Verma, J. Baselga, and D. P. Lane. 2011. Translating p53 into the clinic. *Nature reviews. Clinical oncology* 8: 25-37.
65. Malkin, D., F. P. Li, L. C. Strong, J. F. Fraumeni, Jr., C. E. Nelson, D. H. Kim, J. Kassel, M. A. Gryka, F. Z. Bischoff, M. A. Tainsky, and et al. 1990. Germ line p53 mutations in a familial syndrome of breast cancer, sarcomas, and other neoplasms. *Science* 250: 1233-1238.
66. Jacks, T., L. Remington, B. O. Williams, E. M. Schmitt, S. Halachmi, R. T. Bronson, and R. A. Weinberg. 1994. Tumor spectrum analysis in p53-mutant mice. *Current biology : CB* 4: 1-7.

67. Danovi, D., E. Meulmeester, D. Pasini, D. Migliorini, M. Capra, R. Frenk, P. de Graaf, S. Francoz, P. Gasparini, A. Gobbi, K. Helin, P. G. Pelicci, A. G. Jochemsen, and J. C. Marine. 2004. Amplification of Mdmx (or Mdm4) directly contributes to tumor formation by inhibiting p53 tumor suppressor activity. *Molecular and cellular biology* 24: 5835-5843.
68. Reifemberger, G., L. Liu, K. Ichimura, E. E. Schmidt, and V. P. Collins. 1993. Amplification and overexpression of the MDM2 gene in a subset of human malignant gliomas without p53 mutations. *Cancer research* 53: 2736-2739.
69. Momand, J., D. Jung, S. Wilczynski, and J. Niland. 1998. The MDM2 gene amplification database. *Nucleic acids research* 26: 3453-3459.
70. Mairinger, F. D., R. F. Walter, S. Ting, C. Vollbrecht, J. Kollmeier, S. Griff, T. Hager, T. Mairinger, D. C. Christoph, D. Theegarten, K. W. Schmid, and J. Wohlschlaeger. 2014. Mdm2 protein expression is strongly associated with survival in malignant pleural mesothelioma. *Future oncology* 10: 995-1005.
71. Wasylishen, A. R., and G. Lozano. 2016. Attenuating the p53 Pathway in Human Cancers: Many Means to the Same End. *Cold Spring Harbor perspectives in medicine* 6.
72. Ray-Coquard, I., J. Y. Blay, A. Italiano, A. Le Cesne, N. Penel, J. Zhi, F. Heil, R. Rueger, B. Graves, M. Ding, D. Geho, S. A. Middleton, L. T. Vassilev, G. L. Nichols, and B. N. Bui. 2012. Effect of the MDM2 antagonist RG7112 on the P53 pathway in patients with MDM2-amplified, well-differentiated or

- dedifferentiated liposarcoma: an exploratory proof-of-mechanism study. *The Lancet. Oncology* 13: 1133-1140.
73. Wang, Y., Y. A. Suh, M. Y. Fuller, J. G. Jackson, S. Xiong, T. Terzian, A. Quintas-Cardama, J. A. Bankson, A. K. El-Naggar, and G. Lozano. 2011. Restoring expression of wild-type p53 suppresses tumor growth but does not cause tumor regression in mice with a p53 missense mutation. *The Journal of clinical investigation* 121: 893-904.
 74. Mendrysa, S. M., M. K. McElwee, J. Michalowski, K. A. O'Leary, K. M. Young, and M. E. Perry. 2003. mdm2 Is critical for inhibition of p53 during lymphopoiesis and the response to ionizing irradiation. *Molecular and cellular biology* 23: 462-472.
 75. Alt, J. R., T. C. Greiner, J. L. Cleveland, and C. M. Eischen. 2003. Mdm2 haploinsufficiency profoundly inhibits Myc-induced lymphomagenesis. *The EMBO journal* 22: 1442-1450.
 76. Terzian, T., Y. Wang, C. S. Van Pelt, N. F. Box, E. L. Travis, and G. Lozano. 2007. Haploinsufficiency of Mdm2 and Mdm4 in tumorigenesis and development. *Molecular and cellular biology* 27: 5479-5485.
 77. Eischen, C. M., M. F. Roussel, S. J. Korsmeyer, and J. L. Cleveland. 2001. Bax loss impairs Myc-induced apoptosis and circumvents the selection of p53 mutations during Myc-mediated lymphomagenesis. *Molecular and cellular biology* 21: 7653-7662.

78. Collins, F. S., M. S. Guyer, and A. Charkravarti. 1997. Variations on a theme: cataloging human DNA sequence variation. *Science* 278: 1580-1581.
79. Kruglyak, L., and D. A. Nickerson. 2001. Variation is the spice of life. *Nature genetics* 27: 234-236.
80. Li, Y., W. Chen, E. Y. Liu, and Y. H. Zhou. 2013. Single Nucleotide Polymorphism (SNP) Detection and Genotype Calling from Massively Parallel Sequencing (MPS) Data. *Statistics in biosciences* 5: 3-25.
81. Kuehl, P., J. Zhang, Y. Lin, J. Lamba, M. Assem, J. Schuetz, P. B. Watkins, A. Daly, S. A. Wrighton, S. D. Hall, P. Maurel, M. Relling, C. Brimer, K. Yasuda, R. Venkataramanan, S. Strom, K. Thummel, M. S. Boguski, and E. Schuetz. 2001. Sequence diversity in CYP3A promoters and characterization of the genetic basis of polymorphic CYP3A5 expression. *Nature genetics* 27: 383-391.
82. Cargill, M., D. Altshuler, J. Ireland, P. Sklar, K. Ardlie, N. Patil, N. Shaw, C. R. Lane, E. P. Lim, N. Kalyanaraman, J. Nemesh, L. Ziaugra, L. Friedland, A. Rolfe, J. Warrington, R. Lipshutz, G. Q. Daley, and E. S. Lander. 1999. Characterization of single-nucleotide polymorphisms in coding regions of human genes. *Nature genetics* 22: 231-238.
83. Pastinen, T., R. Sladek, S. Gurd, A. Sammak, B. Ge, P. Lepage, K. Lavergne, A. Villeneuve, T. Gaudin, H. Brandstrom, A. Beck, A. Verner, J. Kingsley, E. Harmsen, D. Labuda, K. Morgan, M. C. Vohl, A. K. Naumova, D. Sinnett, and T. J. Hudson. 2004. A survey of genetic and epigenetic variation affecting human gene expression. *Physiological genomics* 16: 184-193.

84. Lee, P. H., and H. Shatkay. 2008. F-SNP: computationally predicted functional SNPs for disease association studies. *Nucleic acids research* 36: D820-824.
85. Shastry, B. S. 2007. SNPs in disease gene mapping, medicinal drug development and evolution. *Journal of human genetics* 52: 871-880.
86. Iwamoto, T., K. Ikari, T. Nakamura, M. Kuwahara, Y. Toyama, T. Tomatsu, S. Momohara, and N. Kamatani. 2006. Association between PADI4 and rheumatoid arthritis: a meta-analysis. *Rheumatology* 45: 804-807.
87. Guo, X., H. Zheng, C. Mao, E. Guan, and H. Si. 2016. An association and meta-analysis study of 4 SNPs from beta-2 adrenergic receptor (ADRB2) gene with risk of asthma in children. *Asian Pacific journal of allergy and immunology* 34: 11-20.
88. Hunt, R., Z. E. Sauna, S. V. Ambudkar, M. M. Gottesman, and C. Kimchi-Sarfaty. 2009. Silent (synonymous) SNPs: should we care about them? *Methods in molecular biology* 578: 23-39.
89. Menendez, D., O. Krysiak, A. Inga, B. Krysiak, M. A. Resnick, and G. Schonfelder. 2006. A SNP in the flt-1 promoter integrates the VEGF system into the p53 transcriptional network. *Proceedings of the National Academy of Sciences of the United States of America* 103: 1406-1411.
90. Pittman, A. M., S. Naranjo, E. Webb, P. Broderick, E. H. Lips, T. van Wezel, H. Morreau, K. Sullivan, S. Fielding, P. Twiss, J. Vijayakrishnan, F. Casares, M. Qureshi, J. L. Gomez-Skarmeta, and R. S. Houlston. 2009. The colorectal

- cancer risk at 18q21 is caused by a novel variant altering SMAD7 expression. *Genome research* 19: 987-993.
91. Azzam, G. A., A. K. Frank, M. Hollstein, and M. E. Murphy. 2011. Tissue-specific apoptotic effects of the p53 codon 72 polymorphism in a mouse model. *Cell cycle* 10: 1352-1355.
 92. Lu, M., Z. Liu, H. Yu, L. E. Wang, G. Li, E. M. Sturgis, D. G. Johnson, and Q. Wei. 2012. Combined effects of E2F1 and E2F2 polymorphisms on risk and early onset of squamous cell carcinoma of the head and neck. *Molecular carcinogenesis* 51 Suppl 1: E132-141.
 93. Johne, A., I. Roots, and J. Brockmoller. 2003. A single nucleotide polymorphism in the human H-ras proto-oncogene determines the risk of urinary bladder cancer. *Cancer epidemiology, biomarkers & prevention : a publication of the American Association for Cancer Research, cosponsored by the American Society of Preventive Oncology* 12: 68-70.
 94. Sur, I. K., O. Hallikas, A. Vaharautio, J. Yan, M. Turunen, M. Enge, M. Taipale, A. Karhu, L. A. Aaltonen, and J. Taipale. 2012. Mice lacking a Myc enhancer that includes human SNP rs6983267 are resistant to intestinal tumors. *Science* 338: 1360-1363.
 95. Tuupanen, S., J. Yan, M. Turunen, A. E. Gylfe, E. Kaasinen, L. Li, C. Eng, D. A. Culver, M. F. Kalady, M. J. Pennison, B. Pasche, U. Manne, A. de la Chapelle, H. Hampel, B. E. Henderson, L. Le Marchand, S. Hautaniemi, H. Askhtorab, D. Smoot, R. S. Sandler, T. Keku, S. S. Kupfer, N. A. Ellis, C. A. Haiman, J. Taipale,

- and L. A. Aaltonen. 2012. Characterization of the colorectal cancer-associated enhancer MYC-335 at 8q24: the role of rs67491583. *Cancer genetics* 205: 25-33.
96. Pasutto, F., M. Zenkel, U. Hoja, D. Berner, S. Uebe, F. Ferrazzi, J. Schodel, P. Liravi, M. Ozaki, D. Paoli, P. Frezzotti, T. Mizoguchi, S. Nakano, T. Kubota, S. Manabe, E. Salvi, P. Manunta, D. Cusi, C. Gieger, H. E. Wichmann, T. Aung, C. C. Khor, F. E. Kruse, A. Reis, and U. Schlotzer-Schrehardt. 2017. Pseudoexfoliation syndrome-associated genetic variants affect transcription factor binding and alternative splicing of LOXL1. *Nature communications* 8: 15466.
 97. Levine, A. J. 1997. p53, the cellular gatekeeper for growth and division. *Cell* 88: 323-331.
 98. Riley, T., E. Sontag, P. Chen, and A. Levine. 2008. Transcriptional control of human p53-regulated genes. *Nature reviews. Molecular cell biology* 9: 402-412.
 99. Kemp, C. J., T. Wheldon, and A. Balmain. 1994. p53-deficient mice are extremely susceptible to radiation-induced tumorigenesis. *Nature genetics* 8: 66-69.
 100. Grochola, L. F., J. Zeron-Medina, S. Meriaux, and G. L. Bond. 2010. Single-nucleotide polymorphisms in the p53 signaling pathway. *Cold Spring Harbor perspectives in biology* 2: a001032.

101. Hrstka, R., P. J. Coates, and B. Vojtesek. 2009. Polymorphisms in p53 and the p53 pathway: roles in cancer susceptibility and response to treatment. *Journal of cellular and molecular medicine* 13: 440-453.
102. Harris, N., E. Brill, O. Shohat, M. Prokocimer, D. Wolf, N. Arai, and V. Rotter. 1986. Molecular basis for heterogeneity of the human p53 protein. *Molecular and cellular biology* 6: 4650-4656.
103. Thomas, M., A. Kalita, S. Labrecque, D. Pim, L. Banks, and G. Matlashewski. 1999. Two polymorphic variants of wild-type p53 differ biochemically and biologically. *Molecular and cellular biology* 19: 1092-1100.
104. Rosenthal, A. N., A. Ryan, R. M. Al-Jehani, A. Storey, C. A. Harwood, and I. J. Jacobs. 1998. p53 codon 72 polymorphism and risk of cervical cancer in UK. *Lancet* 352: 871-872.
105. Fan, R., M. T. Wu, D. Miller, J. C. Wain, K. T. Kelsey, J. K. Wiencke, and D. C. Christiani. 2000. The p53 codon 72 polymorphism and lung cancer risk. *Cancer epidemiology, biomarkers & prevention : a publication of the American Association for Cancer Research, cosponsored by the American Society of Preventive Oncology* 9: 1037-1042.
106. Zhu, F., M. E. Dolle, T. R. Berton, R. V. Kuiper, C. Capps, A. Espejo, M. J. McArthur, M. T. Bedford, H. van Steeg, A. de Vries, and D. G. Johnson. 2010. Mouse models for the p53 R72P polymorphism mimic human phenotypes. *Cancer research* 70: 5851-5859.

107. Bond, G. L., W. Hu, E. E. Bond, H. Robins, S. G. Lutzker, N. C. Arva, J. Bargonetti, F. Bartel, H. Taubert, P. Wuerl, K. Onel, L. Yip, S. J. Hwang, L. C. Strong, G. Lozano, and A. J. Levine. 2004. A single nucleotide polymorphism in the MDM2 promoter attenuates the p53 tumor suppressor pathway and accelerates tumor formation in humans. *Cell* 119: 591-602.
108. Wo, X., D. Han, H. Sun, Y. Liu, X. Meng, J. Bai, F. Chen, Y. Yu, Y. Jin, and S. Fu. 2011. MDM2 SNP309 contributes to tumor susceptibility: a meta-analysis. *Journal of genetics and genomics = Yi chuan xue bao* 38: 341-350.
109. Asomaning, K., A. E. Reid, W. Zhou, R. S. Heist, R. Zhai, L. Su, E. L. Kwak, L. Blazskowsky, A. X. Zhu, D. P. Ryan, D. C. Christiani, and G. Liu. 2008. MDM2 promoter polymorphism and pancreatic cancer risk and prognosis. *Clinical cancer research : an official journal of the American Association for Cancer Research* 14: 4010-4015.
110. Wo, X., D. Han, H. Sun, Y. Liu, X. Meng, J. Bai, F. Chen, Y. Yu, Y. Jin, and S. Fu. 2011. MDM2 SNP309 contributes to tumor susceptibility: a meta-analysis. *J Genet Genomics* 38: 341-350.
111. Yu, H., Y. J. Huang, Z. Liu, L. E. Wang, G. Li, E. M. Sturgis, D. G. Johnson, and Q. Wei. 2011. Effects of MDM2 promoter polymorphisms and p53 codon 72 polymorphism on risk and age at onset of squamous cell carcinoma of the head and neck. *Mol. Carcinog.* 50: 697-706.

112. Zhuo, W., L. Zhang, B. Zhu, J. Ling, and Z. Chen. 2012. Association of MDM2 SNP309 variation with lung cancer risk: evidence from 7196 cases and 8456 controls. *PloS one* 7: e41546.
113. Hu, Z., H. Ma, D. Lu, J. Qian, J. Zhou, Y. Chen, L. Xu, X. Wang, Q. Wei, and H. Shen. 2006. Genetic variants in the MDM2 promoter and lung cancer risk in a Chinese population. *International journal of cancer. Journal international du cancer* 118: 1275-1278.
114. Zhang, X., X. Miao, Y. Guo, W. Tan, Y. Zhou, T. Sun, Y. Wang, and D. Lin. 2006. Genetic polymorphisms in cell cycle regulatory genes MDM2 and TP53 are associated with susceptibility to lung cancer. *Human mutation* 27: 110-117.
115. Pine, S. R., L. E. Mechanic, E. D. Bowman, J. A. Welsh, S. C. Chanock, P. G. Shields, and C. C. Harris. 2006. MDM2 SNP309 and SNP354 are not associated with lung cancer risk. *Cancer epidemiology, biomarkers & prevention : a publication of the American Association for Cancer Research, cosponsored by the American Society of Preventive Oncology* 15: 1559-1561.
116. Knappskog, S., J. Trovik, J. Marcickiewicz, S. Tingulstad, A. C. Staff, T. E. C. s. g. MoMa, P. Romundstad, K. Hveem, L. Vatten, H. B. Salvesen, and P. E. Lonning. 2012. SNP285C modulates oestrogen receptor/Sp1 binding to the MDM2 promoter and reduces the risk of endometrial but not prostatic cancer. *European journal of cancer* 48: 1988-1996.
117. Knappskog, S., M. Bjornslett, L. M. Myklebust, P. E. Huijts, M. P. Vreeswijk, H. Edvardsen, Y. Guo, X. Zhang, M. Yang, S. K. Ylisaukko-Oja, P. Alhopuro, J. Arola,

- R. A. Tollenaar, C. J. van Asperen, C. Seynaeve, V. Staalesen, R. Chrisanthar, E. Lokkevik, H. B. Salvesen, D. G. Evans, W. G. Newman, D. Lin, L. A. Aaltonen, A. L. Borresen-Dale, G. S. Tell, C. Stoltenberg, P. Romundstad, K. Hveem, J. R. Lillehaug, L. Vatten, P. Devilee, A. Dorum, and P. E. Lonning. 2011. The MDM2 promoter SNP285C/309G haplotype diminishes Sp1 transcription factor binding and reduces risk for breast and ovarian cancer in Caucasians. *Cancer cell* 19: 273-282.
118. Toffoli, G., P. Bion, A. Russo, E. De Mattia, E. Cecchin, C. M. Hattinger, M. Pasello, M. Alberghini, C. Ferrari, K. Scotlandi, P. Picci, and M. Serra. 2009. Effect of TP53 Arg72Pro and MDM2 SNP309 polymorphisms on the risk of high-grade osteosarcoma development and survival. *Clinical cancer research : an official journal of the American Association for Cancer Research* 15: 3550-3556.
119. Post, S. M., A. Quintas-Cardama, V. Pant, T. Iwakuma, A. Hamir, J. G. Jackson, D. R. Maccio, G. L. Bond, D. G. Johnson, A. J. Levine, and G. Lozano. 2010. A high-frequency regulatory polymorphism in the p53 pathway accelerates tumor development. *Cancer cell* 18: 220-230.
120. Liu, G., D. Jiang, S. Shen, and L. Yu. 2012. Murine double minute 2 promoter SNP309 polymorphism and prostate cancer risk: a meta-analysis. *International journal of urology : official journal of the Japanese Urological Association* 19: 914-920.

121. Cotignola, J., J. F. Chou, P. Roy, N. Mitra, K. Busam, A. C. Halpern, and I. Orlow. 2012. Investigation of the effect of MDM2 SNP309 and TP53 Arg72Pro polymorphisms on the age of onset of cutaneous melanoma. *The Journal of investigative dermatology* 132: 1471-1478.
122. Yang, X. I., Y. Zhu, D. Ye, Y. Liu, H. Sun, M. Ruan, and W. Liu. 2016. Association of MDM2 promoter T309G polymorphism with oral cancer risk: A meta-analysis of 3,536 subjects. *Molecular and clinical oncology* 5: 175-180.
123. Ottman, R. 1996. Gene-environment interaction: definitions and study designs. *Preventive medicine* 25: 764-770.
124. Brennan, P. 2002. Gene-environment interaction and aetiology of cancer: what does it mean and how can we measure it? *Carcinogenesis* 23: 381-387.
125. Ryan, S. G. 2003. Regression to the truth: replication of association in pharmacogenetic studies. *Pharmacogenomics* 4: 201-207.
126. Chung, C. C., W. C. Magalhaes, J. Gonzalez-Bosquet, and S. J. Chanock. 2010. Genome-wide association studies in cancer--current and future directions. *Carcinogenesis* 31: 111-120.
127. Easton, D. F., and R. A. Eeles. 2008. Genome-wide association studies in cancer. *Human molecular genetics* 17: R109-115.
128. Figueiredo, J. C., J. P. Lewinger, C. Song, P. T. Campbell, D. V. Conti, C. K. Edlund, D. J. Duggan, J. Rangrej, M. Lemire, T. Hudson, B. Zanke, M. Cotterchio, S. Gallinger, M. Jenkins, J. Hopper, R. Haile, P. Newcomb, J. Potter, J. A. Baron, L. Le Marchand, and G. Casey. 2011. Genotype-environment interactions in

- microsatellite stable/microsatellite instability-low colorectal cancer: results from a genome-wide association study. *Cancer epidemiology, biomarkers & prevention : a publication of the American Association for Cancer Research, cosponsored by the American Society of Preventive Oncology* 20: 758-766.
129. Ramzi, N. H., J. K. Chahil, S. H. Lye, K. Munretnam, K. I. Sahadevappa, S. Velapasamy, N. A. Hashim, S. K. Cheah, G. C. Lim, H. Hussein, M. R. Haron, L. Alex, and L. W. Ler. 2014. Role of genetic & environment risk factors in the aetiology of colorectal cancer in Malaysia. *The Indian journal of medical research* 139: 873-882.
 130. Yang, I. A., J. W. Holloway, and K. M. Fong. 2013. Genetic susceptibility to lung cancer and co-morbidities. *Journal of thoracic disease* 5 Suppl 5: S454-462.
 131. Welsh, M. M., M. R. Karagas, J. K. Kuriger, A. Houseman, S. K. Spencer, A. E. Perry, and H. H. Nelson. 2011. Genetic determinants of UV-susceptibility in non-melanoma skin cancer. *PloS one* 6: e20019.
 132. Azzam, E. I., J. P. Jay-Gerin, and D. Pain. 2012. Ionizing radiation-induced metabolic oxidative stress and prolonged cell injury. *Cancer letters* 327: 48-60.
 133. Fazel, R., H. M. Krumholz, Y. Wang, J. S. Ross, J. Chen, H. H. Ting, N. D. Shah, K. Nasir, A. J. Einstein, and B. K. Nallamothu. 2009. Exposure to low-dose ionizing radiation from medical imaging procedures. *The New England journal of medicine* 361: 849-857.

134. Kaplan, H. S., and M. B. Brown. 1952. A quantitative dose-response study of lymphoid-tumor development in irradiated C 57 black mice. *Journal of the National Cancer Institute* 13: 185-208.
135. Nagar, S., L. E. Smith, and W. F. Morgan. 2005. Variation in apoptosis profiles in radiation-induced genomically unstable cell lines. *Radiation research* 163: 324-331.
136. Narayanan, D. L., R. N. Saladi, and J. L. Fox. 2010. Ultraviolet radiation and skin cancer. *International journal of dermatology* 49: 978-986.
137. Budden, T., and N. A. Bowden. 2013. The role of altered nucleotide excision repair and UVB-induced DNA damage in melanomagenesis. *International journal of molecular sciences* 14: 1132-1151.
138. Spivak, G. 2015. Nucleotide excision repair in humans. *DNA repair* 36: 13-18.
139. Qin, J. Z., V. Chaturvedi, M. F. Denning, P. Bacon, J. Panella, D. Choubey, and B. J. Nickoloff. 2002. Regulation of apoptosis by p53 in UV-irradiated human epidermis, psoriatic plaques and senescent keratinocytes. *Oncogene* 21: 2991-3002.
140. Ichihashi, M., M. Ueda, A. Budiyo, T. Bito, M. Oka, M. Fukunaga, K. Tsuru, and T. Horikawa. 2003. UV-induced skin damage. *Toxicology* 189: 21-39.
141. Skobowiat, C., J. C. Dowdy, R. M. Sayre, R. C. Tuckey, and A. Slominski. 2011. Cutaneous hypothalamic-pituitary-adrenal axis homolog: regulation by ultraviolet radiation. *American journal of physiology. Endocrinology and metabolism* 301: E484-493.

142. Woodworth, C. D., E. Michael, L. Smith, K. Vijayachandra, A. Glick, H. Hennings, and S. H. Yuspa. 2004. Strain-dependent differences in malignant conversion of mouse skin tumors is an inherent property of the epidermal keratinocyte. *Carcinogenesis* 25: 1771-1778.
143. Glick, A., A. Ryscavage, R. Perez-Lorenzo, H. Hennings, S. Yuspa, and N. Darwiche. 2007. The high-risk benign tumor: evidence from the two-stage skin cancer model and relevance for human cancer. *Molecular carcinogenesis* 46: 605-610.
144. Bassi, D. E., and A. J. Klein-Szanto. 2007. Carcinogen-induced animal models of head and neck squamous cell carcinoma. *Current protocols in pharmacology* Chapter 14: Unit 14 12.
145. Hennings, H., A. B. Glick, D. T. Lowry, L. S. Krsmanovic, L. M. Sly, and S. H. Yuspa. 1993. FVB/N mice: an inbred strain sensitive to the chemical induction of squamous cell carcinomas in the skin. *Carcinogenesis* 14: 2353-2358.
146. Mauthe, R. J., V. M. Cook, S. L. Coffing, and W. M. Baird. 1995. Exposure of mammalian cell cultures to benzo[a]pyrene and light results in oxidative DNA damage as measured by 8-hydroxydeoxyguanosine formation. *Carcinogenesis* 16: 133-137.
147. Consortium, E. P. 2012. An integrated encyclopedia of DNA elements in the human genome. *Nature* 489: 57-74.

148. Wong, C. F., L. M. Barnes, L. Smith, C. Popa, M. M. Serewko-Auret, and N. A. Saunders. 2004. E2F6: a member of the E2F family that does not modulate squamous differentiation. *Biochemical and biophysical research communications* 324: 497-503.
149. Liu, G., J. M. Parant, G. Lang, P. Chau, A. Chavez-Reyes, A. K. El-Naggar, A. Multani, S. Chang, and G. Lozano. 2004. Chromosome stability, in the absence of apoptosis, is critical for suppression of tumorigenesis in Trp53 mutant mice. *Nature genetics* 36: 63-68.
150. Russell, J. L., R. L. Weeks, T. R. Berton, and D. G. Johnson. 2006. E2F1 suppresses skin carcinogenesis via the ARF-p53 pathway. *Oncogene* 25: 867-876.
151. Zhang, Y., S. Xiong, Q. Li, S. Hu, M. Tashakori, C. Van Pelt, M. J. You, L. Pagoon, and G. Lozano. 2014. Tissue-specific and age-dependent effects of global Mdm2 loss. *The Journal of pathology* 233: 380-391.
152. Jackson, J. G., and O. M. Pereira-Smith. 2006. Primary and compensatory roles for RB family members at cell cycle gene promoters that are deacetylated and downregulated in doxorubicin-induced senescence of breast cancer cells. *Molecular and cellular biology* 26: 2501-2510.
153. Frank, S. R., M. Schroeder, P. Fernandez, S. Taubert, and B. Amati. 2001. Binding of c-Myc to chromatin mediates mitogen-induced acetylation of histone H4 and gene activation. *Genes & development* 15: 2069-2082.

154. Xu, X., M. Bieda, V. X. Jin, A. Rabinovich, M. J. Oberley, R. Green, and P. J. Farnham. 2007. A comprehensive ChIP-chip analysis of E2F1, E2F4, and E2F6 in normal and tumor cells reveals interchangeable roles of E2F family members. *Genome research* 17: 1550-1561.
155. Lazarus, P., S. N. Sheikh, Q. Ren, S. P. Schantz, J. C. Stern, J. P. Richie, Jr., and J. Y. Park. 1998. p53, but not p16 mutations in oral squamous cell carcinomas are associated with specific CYP1A1 and GSTM1 polymorphic genotypes and patient tobacco use. *Carcinogenesis* 19: 509-514.
156. Sabbatini, P., and F. McCormick. 1999. Phosphoinositide 3-OH kinase (PI3K) and PKB/Akt delay the onset of p53-mediated, transcriptionally dependent apoptosis. *The Journal of biological chemistry* 274: 24263-24269.
157. Gottlieb, T. M., J. F. Leal, R. Seger, Y. Taya, and M. Oren. 2002. Cross-talk between Akt, p53 and Mdm2: possible implications for the regulation of apoptosis. *Oncogene* 21: 1299-1303.
158. Buckland, P. R. 2004. Allele-specific gene expression differences in humans. *Human molecular genetics* 13 Spec No 2: R255-260.
159. Mele, M., P. G. Ferreira, F. Reverter, D. S. DeLuca, J. Monlong, M. Sammeth, T. R. Young, J. M. Goldmann, D. D. Pervouchine, T. J. Sullivan, R. Johnson, A. V. Segre, S. Djebali, A. Niarchou, G. T. Consortium, F. A. Wright, T. Lappalainen, M. Calvo, G. Getz, E. T. Dermitzakis, K. G. Ardlie, and R. Guigo. 2015. Human genomics. The human transcriptome across tissues and individuals. *Science* 348: 660-665.

160. Petryszak, R., M. Keays, Y. A. Tang, N. A. Fonseca, E. Barrera, T. Burdett, A. Fullgrabe, A. M. Fuentes, S. Jupp, S. Koskinen, O. Mannion, L. Huerta, K. Megy, C. Snow, E. Williams, M. Barzine, E. Hastings, H. Weisser, J. Wright, P. Jaiswal, W. Huber, J. Choudhary, H. E. Parkinson, and A. Brazma. 2016. Expression Atlas update--an integrated database of gene and protein expression in humans, animals and plants. *Nucleic acids research* 44: D746-752.
161. Uhlen, M., L. Fagerberg, B. M. Hallstrom, C. Lindskog, P. Oksvold, A. Mardinoglu, A. Sivertsson, C. Kampf, E. Sjostedt, A. Asplund, I. Olsson, K. Edlund, E. Lundberg, S. Navani, C. A. Szigyanto, J. Odeberg, D. Djureinovic, J. O. Takanen, S. Hober, T. Alm, P. H. Edqvist, H. Berling, H. Tegel, J. Mulder, J. Rockberg, P. Nilsson, J. M. Schwenk, M. Hamsten, K. von Feilitzen, M. Forsberg, L. Persson, F. Johansson, M. Zwahlen, G. von Heijne, J. Nielsen, and F. Ponten. 2015. Proteomics. Tissue-based map of the human proteome. *Science* 347: 1260419.
162. Brawand, D., M. Soumillon, A. Necsulea, P. Julien, G. Csardi, P. Harrigan, M. Weier, A. Liechti, A. Aximu-Petri, M. Kircher, F. W. Albert, U. Zeller, P. Khaitovich, F. Grutzner, S. Bergmann, R. Nielsen, S. Paabo, and H. Kaessmann. 2011. The evolution of gene expression levels in mammalian organs. *Nature* 478: 343-348.
163. Breschi, A., S. Djebali, J. Gillis, D. D. Pervouchine, A. Dobin, C. A. Davis, T. R. Gingeras, and R. Guigo. 2016. Gene-specific patterns of expression variation across organs and species. *Genome biology* 17: 151.

164. Qin, J., X. Cong, J. Jin, Z. Chu, X. Gu, and Y. Cai. 2015. Association between MDM2 SNP309 and skin cancer: A meta-analysis of case-control studies. *Journal of dermatological science* 79: 171-173.

Vita

Guadalupe Javier Ortiz IV was born in McAllen, Texas on September 25, 1976, the Son of Graciela and Javier Ortiz. After completing his work at Okeechobee High School, Okeechobee, Florida in 1995, he entered The University of Florida in Gainesville, Florida in August 1998. He received the degree of Bachelor of Science with a major in Wildlife Ecology and Conservation in May 2001. For the next three years, he worked as a research technician in the Department of Biochemistry at The University of Florida. He entered The University of Florida in August 2008. He received the degree of Master of Science in Medical Science August 2010. In August of 2010 he entered The University of Texas MD Anderson Cancer Center UT Health Graduate School of Biomedical Sciences.

Permanent address:

7901 Cambridge Street Apt. 125

Houston, Texas 77054